Table 5 Synchronous metastasis in the liver of patients with pT_2–pT_4 carcinomas and localization type of GnT-V in the specimens

	Total	Synchronous metastasis in the liver	No metastasis
pT_2–pT_4 carcinomas	130	14	116
Negative	41	2	39
Positive	89	12	77
Granular	46	4	42
Diffuse	43	8[a]	35

[a] $P < 0.05$, significantly different from negative staining group

positive staining group was significantly lower than that of patients in the negative staining group ($P = 0.028$). In addition, the survival rate of patients in the granular-type localization group and that of patients in the diffuse-type localization group tended to be lower, but not statistically significant, than that of patients in the negative staining group (Fig. 2b). A summary of the results of the multivariate regression analysis of prognostic factors for pT_2 gallbladder carcinoma is shown in Table 6. In the analysis, GnT-V was found to be a statistically significant independent risk factor compared with other clinicopathological factors.

Biological effects of GnT-V on gallbladder carcinoma cells in in vitro and in vivo tumor models

Cultured gallbladder carcinoma cells (e.g., Mz-ChA-1, TGBC-1-TKB, TGBC-2-TKB, and TGBC-44-TKB (TG44) cells) express high levels of GnT-V (data not shown). To investigate the biological effects of GnT-V on gallbladder carcinoma cells, a siRNA of GnT-V for suppressing GnT-V expression was introduced into TG44 cells using a retrovirus vector. As shown in Fig. 3a, variable suppression levels of GnT-V were observed in each of the established clones. Based on the protein level analysis, GnT-V activities, and lectin blot of PHA-L, 3 clones were selected for the in vitro and in vivo experiments. TG44-siR-H represented the highest values, whereas TG44-siR-L represented the lowest values. TG44-siR-M represented the intermediate values (Fig. 3a).

In vitro cell growth was fastest for the TG44-siR-H with higher GnT-V expression, the level of which is comparable to that of the original cells (Fig. 3a). On the other hand, in vitro cell growth was slow for the TG44-siR-L with lower GnT-V expression. The TG44-siR-M represented the intermediate growth speed. Similar to the in vitro growth, the TG44-siR-H represented rapid growth in the subcutaneous xenografted tumor model but TG44-siR-L represented slow growth (Fig. 3b). Histopathology, the subcutaneous tumor of TG44-siR-H yielded a high density of microvessels recognized by CD31 compared with those of TG44-siR-L and TG44-siR-M (Fig. 3b).

To mimic the clinical aggressiveness of gallbladder carcinoma cells with GnT-V expression, a persplenic hepatometastatic tumor model was developed using TG44-siR-H, TG44-siR-L, and TG44-siR-M cells. Seven days after persplenic injection of the cells, establishment of hepatometastasis was confirmed using the IVIS imaging

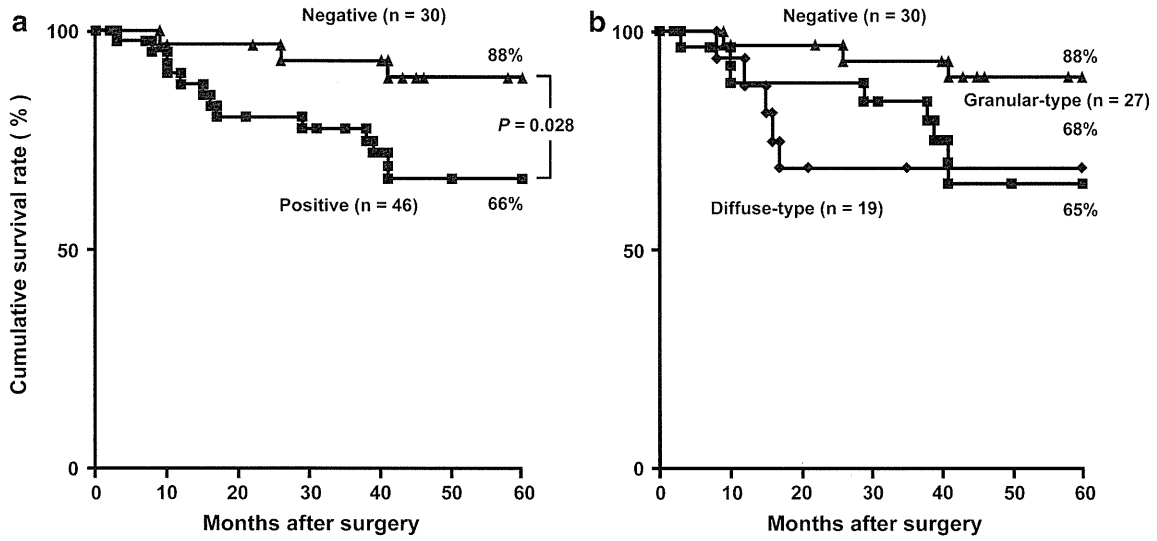

Fig. 2 **a** Relationships between postsurgical survival outcome and GnT-V expression status at the deepest invading sites in the surgical specimens of pT_2 gallbladder carcinoma as shown by Kaplan–Meier survival curves. The 76 curative resection cases of pT_2 gallbladder carcinoma were divided into 2 groups based on the GnT-V expression status ($P = 0.028$, log-rank test). **b** Relationship between postsurgical survival outcome and GnT-V localization-types. Cases showing positive staining were further divided into 2 groups based on the GnT-V localization types, that is, granular- and diffuse-type localization groups. However, there were no significant differences among the 3 groups

Table 6 Multivariate analysis of prognotic factors

Variable	Hazard ratio	C.L.	*P* value
GnT-V	4.82	1.1–21.2	0.038
N	0.82	0.2–8.4	0.780
Histological	2.53	0.7–9.1	0.155
Ly	1.62	0.3–7.9	0.548
Vy	0.45	0.1–1.7	0.244
Pn	0.98	0.2–4.2	0.982

system (Fig. 3c). Tumor volume in the intraperitoneal cavity was assessed using this imaging system which visualizes viable tumor cells as photon intensity (Fig. 3c). Regarding the time-course of change shown in Fig. 3c, the average photon intensity (total flux) was significantly increased in the mice bearing either TG44-siR-H or TG44-siR-M compared with that in the mice bearing TG44-siR-L. Correlating with the observed tumor aggressiveness, the survival period of the TG44-siR-H group (median survival period, 34 days) was significantly shorter than that of the TG44-siR-M group (median survival period, 60 days) and that of the TG44-siR-L group (all mice were alive at the end point of the observation period) (Fig. 3c).

Discussion

The major findings of this study are that the GnT-V protein levels were increased in the tissue specimens of gallbladder carcinoma compared with the GnT-V protein levels in the tissue specimens of normal gallbladder and that alteration in the subcellular localization of GnT-V is closely associated with the biological aspects of gallbladder carcinoma (e.g., aggressiveness to form distant organ metastasis).

The prognosis of pT_2 gallbladder carcinoma is not necessarily favorable despite a theoretical advantage for the carcinoma not invading the perimuscular connective tissues and not extending beyond the serosa or into the liver. This may be because approximately half of the patients had malignant infiltration into the lymphatic, venous, and perineural spaces, and the frequency of lymph node metastasis was 50 % [7, 33]. In this study, the diffuse-type localization of GnT-V at the deepest invading sites correlated with neither histological grade nor parameters of clinicopathological malignancies in the 76 curative resection cases of pT_2 gallbladder carcinoma. Because of the poor association of the expression level with the clinicopathological findings of pT_2 gallbladder carcinoma, the expression levels of GnT-V at the deepest invading sites may be considered to be an independent prognostic marker for pT_2 gallbladder carcinoma, as shown on the multivariate regression analysis (Table 6).

The regulatory basis for the diffuse-type localization on GnT-V immunohistochemistry of has not yet been well elucidated. The proportion of the diffuse-type localization was increased in parallel to the clinical stages of the disease (Table 1). Carcinoma cells at advanced stages are phenotypically different from their counterparts at early stages in their expression of mucin glycoproteins [34] and *N*-Acetylgalactosaminyltransferases (GalNAc-T family enzymes) [26]. Moreover, in relation to the presence of cytoplasmic or stromal localization of MUC1 mucin on immunohistochemistry, which was reported in the cases of pT_2 gallbladder carcinoma with high metastatic potential [9, 35], it has been hypothesized that mucin proteolysis takes place in vivo [36, 37]. A previous study has provided in vitro evidence that MUC1 mucin is cleaved by a metalloprotease(s) [38]. Metastatic gallbladder carcinoma cells may include cells with high levels of this kind of protease(s) mediating the GnT-V proteolysis. Taken together, these phenotypic changes affect the biological behavior of carcinoma cells with an increased metastatic potential.

It is also possible that alterations in the subcellular localization of GnT-V may be simply associated with the status of tumor differentiation and caused by loss of functional differentiation of the carcinoma cells, that is, the failure to establish or maintain the polar expression of normal epithelial localization of this enzyme. The diffuse-type localization of GnT-V in gallbladder carcinoma indicates a reorganization of the Golgi apparatus elements in the carcinoma cells as reported previously [39]. Therefore, the processing and targeting pathway of GnT-V may be defective in the cells. However, in cases of pT_2 gallbladder carcinoma, there was no strong correlation between histological grade (tumor differentiation), that is, papillary, tubular, or poorly differentiated adenocarcinoma, and the expression level of GnT-V at the deepest invading sites (Table 3), indicating that diffuse-type localization cannot be explained solely by differences in the histological grade of pT_2 carcinoma. Nevertheless, the expression level of GnT-V on immunohistochemistry may be a useful biological tool to scale the functional differentiation of pT_2 gallbladder carcinoma cells.

Malignant transformation of glandular epithelia is accompanied by alterations in the biochemical and biological characteristics of glycoproteins. In this study, the mechanism underlying the positive correlation between metastasis and GnT-V expression in pT_2 gallbladder carcinoma can be speculated on by the branching of asparagine-linked oligosaccharides, which is shown to regulate the metastatic potential of carcinoma cells [40]. The β1–6 branching structure, a product of GnT-V, is a good substrate for the attachment of poly-*N*-acetyllactosamine, whose synthesis is controlled by the complemental branch

specificity of i-extension enzyme and 1–4 galactosyltransferase I [41]. This structure is preferentially fucosylated to form sialyl Lewis X, a ligand for selectin in vascular endothelial cells. The level of poly *N*-acetyllactosamine is increased in highly metastatic colon carcinoma cells [42] and that of sialyl Lewis X expression is correlated with poor survival in human colon cancer patients [43, 44]. From these points, GnT-V may induce tumor metastasis through the formation of sialyl Lewis X on the tumor cell surface.

However, in several types of cancers, GnT-V expression correlated inversely with the patient survival outcome [20, 21]. It has been postulated that involvement of GnT-V in tumor biology depends on whether its original organ tissues consist of β1-6 branching of *N*-linked oligosaccharides [20]. When cancers originate from tissues expressing no expression of β1-6 branching oligosaccharides, the induction of GnT-V expression is associated with malignant potential of the cancer cells [18]. On the other hand, when cancers originate from tissues expressing β1-6 branching oligosaccharides, the presence of GnT-V expression is an indicator of good prognosis [20]. Therefore, it should be stressed that the biological significance of GnT-V among cancers is uneven depending on the expression status of GnT-V and β1-6 branching oligosaccharides in original organ tissues. In this study, since normal gallbladder epithelia show no or only trace expression of GnT-V (Table 1), it is likely that the induction of GnT-V expression in gallbladder carcinoma is associated with the observed malignant behaviors of the cancer cells (Tables 4, 5).

Moreover, GnT-V functions as an angiogenesis inducer that has a completely different function from the original function of glycosyltransferase [17]. A secreted type of GnT-V protein itself promotes angiogenesis in vitro and in vivo [30, 45]. These findings provide novel information on the interrelationship among GnT-V, tumor growth and metastasis. In this study, supporting the angiogenesis function of GnT-V, the microvessel density was significantly higher in the tissue specimens of pT_2 gallbladder carcinoma showing positive staining than in those showing negative staining (Fig. 1c). In the subcutaneous tumor models, tumor growth was significantly more rapid for the cells with higher GnT-V expression than for those with lower GnT-V expression. Similar to the clinical specimens, the density was significantly increased in the tumors consisting of cells with higher GnT-V expression than in those consisting of cells with lower GnT-V expression (Fig. 3b). Angiogenesis is the first regulatory step of tumor progression. As shown in the hepatometastatic tumor models (Fig. 3c), the progression of metastatic tumor cells in the liver was significantly more rapid in cells with higher GnT-V expression than in those with lower GnT-V expression. Based on the above-mentioned results, the malignant phenotype can, therefore, be blocked by a GnT-V inhibitor. Swainsonine, a potent GnT-V inhibitor, reduces tumor metastasis and tumor solid growth in mice [46, 47].

Fig. 3 Biological effects of GnT-V on gallbladder carcinoma cells in ▶ in vitro and in vivo tumor models. **A** Construction of GnT-V knockdown gallbladder carcinoma cells by siRNA, as described in the "Materials and Methods" section. Three clones (i.e., TG44-siR-H, TG44-siR-M, and TG44-siR-L, were selected based on the immunoblot analysis of GnT-V (**a**), and subjected to in vitro assays, namely, GnT-V enzyme activity measurement (**b**), the lectin blotting (**c**), and tumor cell growth assay (**d**). **B** Subcutaneous tumors were seeded in immunodeficient mice using TG44-siR-H, TG44-siR-M, and TG44-siR-L (**a**), as described in the "Materials and Methods" section. Each group consisted of 5 animals. Tumor size was measured every other 4 days (**b**), and tumor volume (mm^3) was calculated as 0.5× longest diameter × width^2. Tumor volumes are presented as mean ± SE of 5 mice for each group. Significant differences between the groups are indicated by $*P < 0.05$ and $**P < 0.01$. CD31 immunostaining in tumor tissue sections (**a**) and quantification of microvessel density (**c**). *Bars* 100 μm. *Columns* and *bars* represent means and SE of the microvessel densities in each group, respectively. Quantification of data of microvessel density in the subcutaneous tumor sections was performed. A tumor tissue section was prepared from each of the 5 mice in the TG44-siR-H-, TG44-siR-M-, and TG44-siR-L-implanted groups. Five photographs were taken for each tissue section and then analyzed. Microvessels showing CD31 immunoreactivity were counted. Microvessel density for each of the 5 photographs of the tissue section was averaged, and the averaged densities of the above 3 groups (5 mice in each group) were compared. Significant differences between the groups are indicated by $*P < 0.05$ and $**P < 0.01$. **C** A persplenic hepatometastatic tumor model was developed in immunodeficient mice using TG44-siR-H, TG44-siR-L, and TG44-siR-M, all of which express luciferase, as described in the "Materials and Methods" section. Each group consisted of 5 mice. Sequential in vivo whole-body imaging of tumor progression was monitored over time using the IVIS imaging system (**a**). Panels depict 3 representative mice from each group. Time-course changes in the quantification of tumor bioluminescence were determined. Points, mean area of bioluminescence for live intact mice in each group ($n = 5$); *Bars* SE. Significant differences between groups are indicated by $**P < 0.01$ (**b**). The survival outcome of each group of mice with hepatometastatic tumors was assessed using Kaplan–Meier survival curves (**c**). The survival period of the TG44-siR-H group (median survival period, 34 days) was significantly shorter than that of the TG44-siR-M group (median survival period, 60 days) and that of the TG44-siR-L group (all mice were alive at the end point of the observation period). The differences were statistically significant according to the log-rank test ($*P < 0.05$ and $**P < 0.01$) (**c**)

In summary, the expression of GnT-V at the protein level is up-regulated in gallbladder carcinoma tissues and the immunohistochemical expression level of GnT-V in the subserosal layer of pT_2 gallbladder carcinoma is correlated with aggressiveness of the disease, such as the tendency to form distant recurrences, and with postsurgical survival. Moreover, in the in vitro and in vivo experiments using the gallbladder carcinoma cells, the expression levels of GnT-V in the cells were positively correlated with malignant behaviors, such as rapid cell growth, potent angiogenic capability, and potent metastatic potential. Taken together, the expression levels of GnT-V may serve as a unique biological feature associated with the malignant behavior

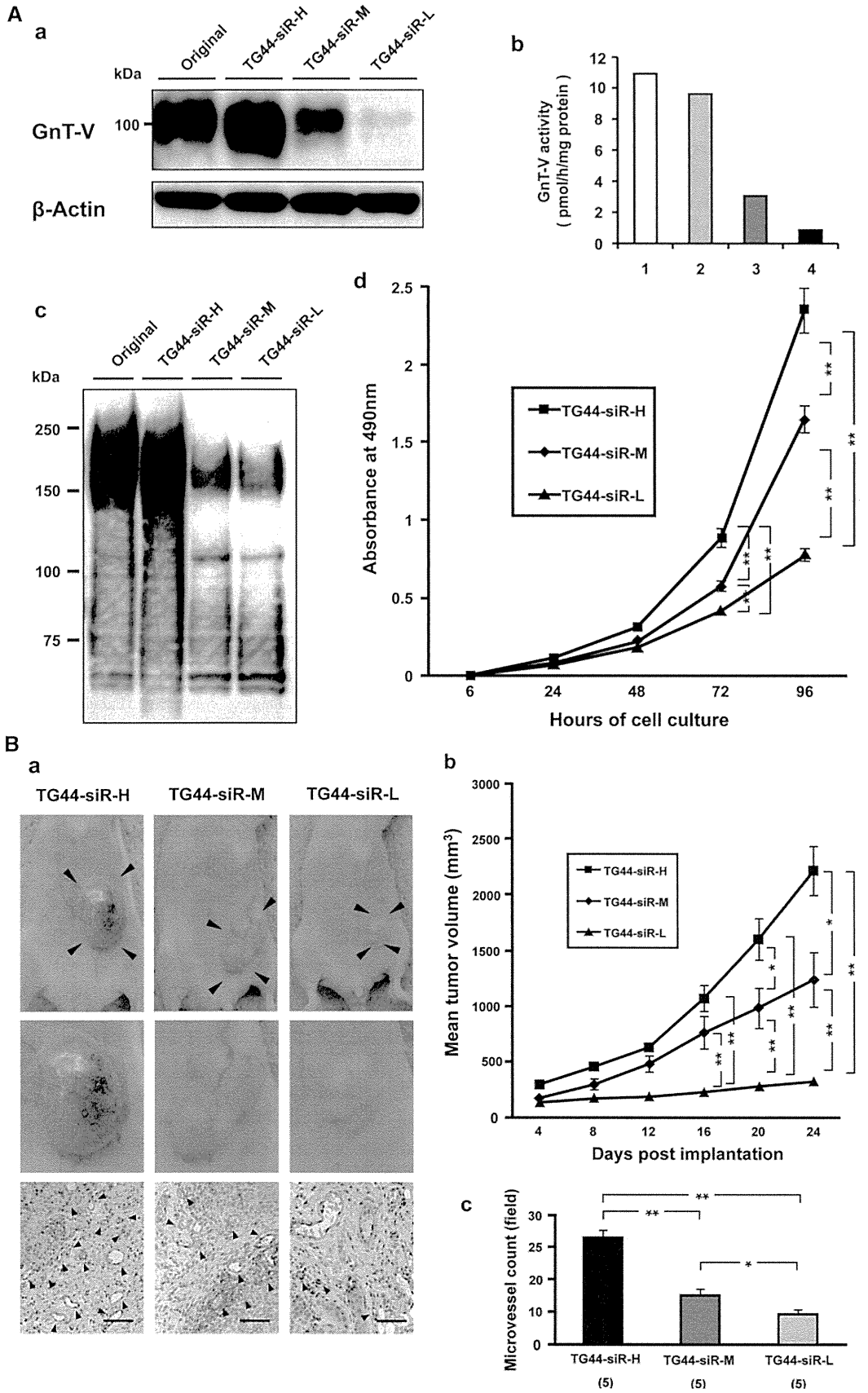
A
a
Original
TG44-siR-H
TG44-siR-M
TG44-siR-L
kDa
GnT-V
100
β-Actin
b
GnT-V activity
(pmol/h/mg protein)
12
10
8
6
4
2
0
1
2
3
4
c
Original
TG44-siR-H
TG44-siR-M
TG44-siR-L
kDa
250
150
100
75
d
Absorbance at 490nm
2.5
2
1.5
1
0.5
0
TG44-siR-H
TG44-siR-M
TG44-siR-L
6
24
48
72
96
Hours of cell culture
B
a
TG44-siR-H
TG44-siR-M
TG44-siR-L
b
Mean tumor volume (mm3)
3000
2500
2000
1500
1000
500
0
TG44-siR-H
TG44-siR-M
TG44-siR-L
4
8
12
16
20
24
Days post implantation
c
Microvessel count (field)
30
25
20
10
0
TG44-siR-H
(5)
TG44-siR-M
(5)
TG44-siR-L
(5)

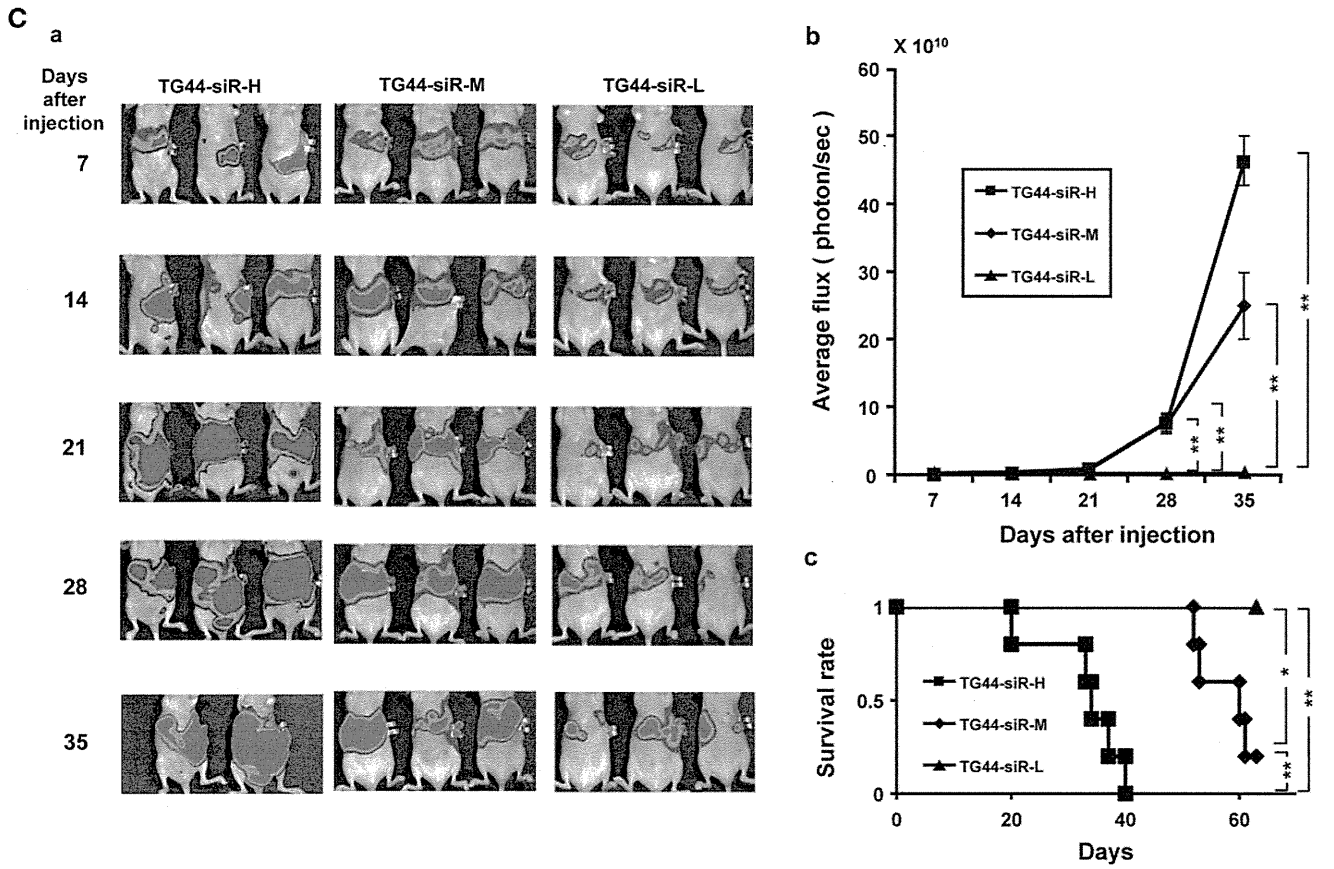

Fig. 3 continued

of gallbladder carcinoma and may be useful in identifying patients in need of closer follow-up and more aggressive treatment.

Acknowledgments Grant support: This work was supported in part by Grants-in-Aid for Scientific Research from the Ministry of Education, Culture, Sports, Science and Technology, Japan (Nos. 22390379, 22591530, 23390318, 23659659, 24390323).

Conflict of interest The authors declare that they have no conflict of interest.

References

1. Ruckert JC, Ruckert RI, Gellert K, Hecker K, Muller JM. Surgery for carcinoma of the gallbladder. Hepatogastroenterology. 1996;43:527–33.
2. Cubertafond P, Gainant A, Cucchiaro G. Surgical treatment of 724 carcinomas of the gallbladder. Results of the French Surgical Association Survey. Ann Surg. 1994;219:275–80.
3. Oertli D, Herzog U, Tondelli P. Primary carcinoma of the gallbladder: operative experience during a 16-year period. Eur J Surg. 1993;159:415–20.
4. Gall FP, Kockerling F, Scheele J, Schneider C, Hohenberger W. Radical operations for carcinoma of the gallbladder: present status in Germany. World J Surg. 1991;15:328–36.
5. Donohue JH, Nagorney DM, Grant CS, Tsushima K, Ilstrup DM, Adson MA. Carcinoma of the gallbladder. Does radical resection improve outcome? Arch Surg. 1990;125:237–41.
6. Ouchi K, Owada Y, Matsuno S, Sato T. Prognostic factors in the surgical treatment of gallbladder carcinoma. Surgery. 1987;101:731–7.
7. Yamaguchi K, Chijiiwa K, Saiki S, Nishihara K, Takashima M, Kawakami K, et al. Retrospective analysis of 70 operations for gallbladder carcinoma. Br J Surg. 1997;84:200–4.
8. Todoroki T, Kawamoto T, Takahashi Y, Takada Y, Koike N, Otsuka M, et al. Treatment of gallbladder cancer by radical resection. Br J Surg. 1999;86:622–7.
9. Kawamoto T, Shoda J, Irimura T, Miyahara N, Furukawa M, Ueda T, et al. Expression of MUC1 mucins in the subserosal layer correlates with post-surgical prognosis of pT_2 carcinoma of the gallbladder. Clin Cancer Res. 2001;7:1333–42.
10. Hart GW, Copeland RJ. Glycomics hits the big time. Cell. 2010;143:672–6.
11. Dennis JW, Laferte S, Waghorne C, Breitman ML, Kerbel RS. Beta 1–6 branching of Asn-linked oligosaccharides is directly associated with metastasis. Science. 1987;236:582–5.
12. Miyoshi E, Nishikawa A, Ihara Y, Gu J, Sugiyama T, Hayashi N, et al. *N*-Acetylglucosaminyltransferase III and V messenger RNA levels in LEC rats during hepatocarcinogenesis. Cancer Res. 1993;53:3899–902.
13. Lau KS, Dennis JW. *N*-glycans in cancer progression. Glycobiology. 2008;18:750–60.
14. Granovsky M, Fata J, Pawling J, Muller WJ, Khokaha R, Dennis JW. Supression of tumor growth and metastasis in Mgat5-deficient mice. Nat Med. 2000;6:306–12.

15. Dennis JW, Nabi IR, Demetriou M. Metabolism, cell surface organization, and disease. Cell. 2009;139:1229–41.
16. Ihara S, Miyoshi E, Ko JH, Murata K, Nakahara S, Honke K, et al. Prometastatic effect of N-Acetylglucosaminyltransferase V is due to modification and stabilization of active matriptase by adding beta 1–6 GlcNAc branching. J Biol Chem. 2002;277:16960–7.
17. Saito T, Miyoshi E, Sasai K, Nakano N, Eguchi H, Honke K, et al. A secreted type of beta 1,6-*N*-Acetylglucosaminyltransferase V (GnT-V) induces tumor angiogenesis without mediation of glycosylation: a novel function of GnT-V distinct from the original glycosyltransferase activity. J Biol Chem. 2002;277:17002–8.
18. Murata K, Miyoshi E, Kameyama M, Ishikawa O, Kabuto T, Sasaki Y, et al. Expression of *N*-Acetylglucosaminyltransferase V in colorectal cancer correlates with metastasis and poor prognosis. Clin Cancer Res. 2000;6:1772–7.
19. Perng GS, Shoreibah M, Margitich I, Pierce M, Fregien N. Expression of *N*-Acetylglucosaminyltransferase V mRNA in mammalian tissues and cell lines. Glycobiology. 1994;4:867–71.
20. Dosaka-Akita H, Miyoshi E, Suzuki O, Itoh T, Katoh H, Taniguchi N. Expression of *N*-Acetylglucosaminyltransferase V is associated with prognosis and histology in non-small cell lung cancers. Clin Cancer Res. 2004;10:1773–9.
21. Ishimura H, Takahashi T, Nakagawa H, Nishimura S, Arai Y, Horikawa Y, et al. N-Acetylglucosaminyltransferase V and beta 1–6 branching N-linked oligosaccharides are associated with good prognosis of patients with bladder cancer. Clin Cancer Res. 2006;12:2506–11.
22. Handerson T, Pawelek JM. Beta 1,6-branched oligosaccharides and coarse vesicles: a common, pervasive phenotype in melanoma and other human cancers. Cancer Res. 2003;63:5363–9.
23. Fleming ID, Cooper JS, Henson DE, Hutter RVP, Kennedy BJ, Murphy GP, O'sullivan B, Sobin LH, Yarbro JW, editors. AJCC cancer staging manual. 5th ed. Philadelphia: Lippincott-Raven; 1997.
24. Knuth A, Gabbert H, Dippold W, Klein O, Sachsse W, Bitter-Suermann D, et al. Biliary adenocarcinoma. Characterisation of three new human tumor cell lines. J Hepatol. 1985;1:579–96.
25. Koike N, Todoroki T, Kawamoto T, Yoshida S, Kashiwagi H, Fukao K, et al. The invasion potentials of human biliary tract carcinoma cell lines: correlation between invasiveness and morphologic characteristics. Int J Oncol. 1998;13:1269–74.
26. Miyahara N, Shoda J, Kawamoto T, Furukawa M, Ueda T, Todoroki T, et al. Expression of UDP-*N*-Acetyl-alpha-D-galactosamine-polypeptide *N*-Acetylgalactosaminyltransferase isozyme 3 in the subserosal layer correlates with postsurgical survival of pathological tumor stage 2 carcinoma of the gallbladder. Clin Cancer Res. 2004;10:2090–9.
27. Weidner N, Semple JP, Welch WR, Folkman J. Tumor angiogenesis and metastasis-correlation in invasive breast carcinoma. N Engl J Med. 1991;324:1–8.
28. Inamori K, Gu J, Ohira M, Kawasaki A, Nakamura Y, Nakagawa T, et al. High expression of *N*-Acetylglucosaminyltransferase V in favorable neuroblastomas: Involvement of its effect on apotosis. FEBS Lett. 2006;580:627–32.
29. Nabekura T, Otsu M, Nagasawa T, Nakauchi H, Onodera M. Potent vaccine therapy with dendritic cells genetically modified by the gene-silencing-resistant retroviral vector GCDNsap. Mol Ther. 2006;13:301–9.
30. Suzuki A, Obi K, Urabe T, Hayakawa H, Yamada M, Kaneko S, et al. Feasibility of ex vivo gene therapy for neurological disorders using the new retroviral vector GCDNsap packaged in the vesicular stomatitis virus G protein. J Neurochem. 2002;82:953–60.
31. Taniguchi N, Miyoshi E, Ko JH, Ikeda Y, Ihara Y. Implication of *N*-Acetylglucosaminyltransferases III and V in cancer: gene regulation and signaling mechanism. Biochim Biophys Acta. 1999;1455:287–300.
32. Ichihara H, Funamoto K, Matsushita T, Matsumoto Y, Ueoka R. Histological bioanalysis for therapeutic effects of hybrid liposomes on the hepatic metastasis of colon carcinoma in vivo. Int J Pharm. 2010;394:174–8.
33. Tsukada K, Hatakeyama K, Kurosaki I, Uchida K, Shirai Y, Muto T, et al. Outcome of radical surgery for carcinoma of the gallbladder according to the TNM stage. Surgery. 1996;120:816–21.
34. Matsushita Y, Cleary KR, Ota DM, Hoff SD, Irimura T. Syalyldimetric Lewis-X antigen expressed on mucin-like glycoproteins in colorectal cancer metastasis. Lab Invest. 1990;63:780–91.
35. Kawamoto T, Shoda J, Miyahara N, Suzuki H, Furukawa M, Todoroki T, et al. Expression of MUC1 recognized by a monoclonal antibody MY.1E12 is a useful biomarker for tumor aggressiveness of carcinoma of the gallbladder. Clin Exp Metastasis. 2004;21:353–62.
36. Zhang K, Baeckstrom D, Brevinge H, Hansson GC. Secreted MUC1 mucins lacking their cytoplasmic part and carrying sialylLewis a and x epitopes from a tumor cell line and sera of colon carcinoma patients can inhibit HL-60 leukocyte adhesion to E-selectin-expressing endothelial cells. J Cell Biochem. 1996;60:538–49.
37. Treon SP, Maimonis P, Bua D, Young G, Raje N, Mollick J, et al. Elevated soluble MUC1 levels and decreased anti-MUC1 antibody levels in patients with multiple melanoma. Blood. 2000;96:3147–53.
38. Thathiah A, Blobel CP, Carson DD. Tumor necrosis factor-α converting enzyme/ADAM 17 mediates MUC1 shedding. J Biol Chem. 2003;278:3386–94.
39. Taatjes DJ, Roth J, Weinstein J, Paulson JC, Shaper NL, Shaper JH. Codistribution of galactosyl- and sialyltransferase: reorganization of trans Golgi apparatus elements in hepatocytes in intact liver and cell culture. Eur J Cell Biol. 1987;44:187–94.
40. Pierce M, Buckhaults P, Chen L, Fregien N. Regulation of *N*-acetylglucosaminyltransferase V and Asn-linked oligosaccharide beta (1,6) branching by a growth factor signaling pathway and effects on cell adhesion and metastatic potential. Glycoconj J. 1997;14:623–30.
41. Ujita M, McAuliffe J, Hindsgaul O, Sasaki K, Fukuda MN, Fukuda M. Poly-*N*-acetyllactosamine synthesis in branched *N*-glycans is controlled by complemental branch specificity of I-extension enzyme and beta1, 4-galactosyltransferase I. J Biol Chem. 1999;274:16717–26.
42. Saitoh O, Wang WC, Lotan R, Fukuda M. Differential glycosylation and cell surface expression of lysosomal membrane glycoproteins in sublines of a human colon cancer exhibiting distinct metastatic potentials. J Biol Chem. 1992;267:5700–11.
43. Nakamori S, Kameyama M, Imaoka S, Furukawa H, Ishikawa O, Sasaki Y, et al. Increased expression of sialyl Lewisx antigen correlates with poor survival in patients with colorectal carcinoma: clinicopathological and immunohistochemical study. Cancer Res. 1993;53:3632–7.
44. Shimodaira K, Nakayama J, Nakamura N, Hasebe O, Katsuyama T, Fukuda M. Carcinoma-associated expression of core 2 beta-1,6-*N*-Acetylglucosaminyltransferase gene in human colorectal cancer: role of *O*-glycans in tumor progression. Cancer Res. 1997;57:5201–6.
45. Nakahara S, Saito T, Kondo N, Moriwaki K, Noda K, Ihara S, et al. A secreted type of β1,6 *N*-acetylglucosaminyltransferase V (GnT-V), a novel angiogenesis inducer, is regulated by γ-secretase. FASEB J. 2006;20:2451–9.
46. Dennis JW. Effects of swainsonine and polycytidylic acid on murine tumor cell growth and metastasis. Cancer Res. 1986;46:5131–6.
47. Goss PE, Reid CL, Bailey D, Dennis JW. Phase IB clinical trial of the oligosaccharide processing inhibitor swainsonone in patients with advanced malignancies. Clin Cancer Res. 1997;3:1077–86.

Liver INTERNATIONAL
OFFICIAL JOURNAL OF THE INTERNATIONAL ASSOCIATION FOR THE STUDY OF THE LIVER

Liver International ISSN 1478-3223

ORIGINAL ARTICLE

Fetuin-A negatively correlates with liver and vascular fibrosis in nonalcoholic fatty liver disease subjects

Motoya Sato[1,*], Yoshihiro Kamada[1,2,*], Yuri Takeda[1], Sachiho Kida[1], Yuka Ohara[1], Hironobu Fujii[1], Maaya Akita[1], Kayo Mizutani[1], Yuichi Yoshida[2], Makoto Yamada[3], Hidetaka Hougaku[4], Tetsuo Takehara[2] and Eiji Miyoshi[1]

1 Department of Molecular Biochemistry & Clinical Investigation, Osaka University, Graduate School of Medicine, Suita, Osaka, Japan
2 Department of Gastroenterology and Hepatology, Osaka University, Graduate School of Medicine, Suita, Osaka, Japan
3 aMs New Otani Clinic, Osaka, Osaka, Japan
4 Nara Institute of Science and Technology, Ikoma, Nara, Japan

Keywords
BAMBI – IMT – NASH/NAFLD – TGF-β1

Abbreviations
BAMBI, bone morphogenic protein and activin membrane-bound inhibitor; CHE, choline esterase; FBG, fasting blood glucose; GGT, γ-glutamyl transpeptidase; Hb, haemoglobin; HSC, hepatic stellate cell; IFG, impaired fasting glucose; IMT, intima media thickness; Mets, metabolic syndrome; NAFLD, nonalcoholic fatty liver disease; NASH, nonalcoholic steatohepatitis; NGSP, National Glycohemoglobin Standardization Program; sBP, systolic blood pressure; T-Chol, total cholesterol; TGF-β1, transforming growth factor-β1; TG, triglyceride; TLR4, toll-like receptor 4; TNF-α, tumour necrosis factor-α; TβRII, TGF- receptor type II.

Correspondence
Eiji Miyoshi, MD, PhD, Department of Molecular Biochemistry & Clinical Investigation, Osaka University Graduate School of Medicine, 1-7 Yamada-oka, Suita, Osaka 565-0871, Japan
Tel: +81-6-6879-2590
Fax: +81-6-6879-2590
e-mail: emiyoshi@sahs.med.osaka-u.ac.jp

Received 3 October 2013
Accepted 26 January 2014

DOI:10.1111/liv.12478

Abstract

Background & Aims: Fetuin-A (α2HS-glycoprotein), a liver secretory glycoprotein, is known as a transforming growth factor (TGF)-β1 signalling inhibitor. Serum fetuin-A concentration is associated with nonalcoholic fatty liver disease (NAFLD) and cardiovascular disease. However, the usefulness of serum fetuin-A as a predictive fibrosis biomarker in NAFLD patients remains unclear. In this study, we investigated the relationship between circulating fetuin-A levels and fibrosis-related markers [platelet count, NAFLD fibrosis score and carotid intima media thickness (IMT)] in subjects with NAFLD. *Methods:* A total of 295 subjects (male, 164; female, 131) who received medical health check-ups were enrolled in this study. NAFLD was diagnosed using abdominal ultrasonography. Serum fetuin-A was measured by ELISA. IMT was assessed using a high-resolution ultrasound scanner. Using recombinant human fetuin-A, we investigated the effects of fetuin-A on hepatic stellate cells, which play a pivotal role in the process of hepatic fibrosis. *Results:* Serum fetuin-A concentration was significantly correlated with platelet count ($R = 0.19$, $P < 0.01$), NAFLD fibrosis score ($R = -0.25$, $P < 0.01$) and mean IMT ($R = -0.22$, $P < 0.01$). Multivariate analyses revealed that the fetuin-A concentration is a significant and independent determinant of platelet count, NAFLD fibrosis score and mean IMT. Recombinant fetuin-A suppressed TGF-β1 signalling and fibrosis-related gene expression and increased the expression of TGF-β1 pseudoreceptor bone morphogenic protein and activin membrane-bound inhibitor (BAMBI). *Conclusions:* Serum fetuin-A level is associated with liver/vessel fibrosis-related markers in NAFLD patients. Circulating fetuin-A could be a useful serum biomarker for predicting liver and vascular fibrosis progression in NAFLD patients.

Nonalcoholic fatty liver disease (NAFLD) is among the most common causes of chronic liver disease in the world and is a growing medical problem in industrialized countries (1). A wide spectrum of hepatic histological changes has been observed in NAFLD, ranging from simple steatosis, which is generally nonprogressive, to nonalcoholic steatohepatitis (NASH). A proportion of patients with NASH develop cirrhosis and hepatocellular carcinoma (2). About 30% of the general population has NAFLD and up to 5% of this population has NASH (3–5). To evaluate liver disease progression in NAFLD patients, liver biopsy remains the gold standard for diagnosing NASH and grading the severity of liver damage

*These authors contributed equally to this study.

(6, 7). However, invasive liver biopsy is not suitable as a large-scale diagnostic test, and this, in turn, restricts therapeutic interventions (8).

NAFLD is a hepatic manifestation of the metabolic syndrome (Mets) and appears to be an almost indispensable prerequisite for Mets development, including development of type 2 diabetes mellitus (DM) and cardiovascular disease (CVD) (9–11). A recent systematic review indicated that NAFLD patients are prone to CVD, independent of Mets (12). In addition, many studies have demonstrated that the presence of NAFLD is an independent risk factor for progression of atherosclerotic disease (13–15). Atherosclerotic disease reportedly plays an important role in the natural course of NAFLD (16). Therefore, there is an urgent need to develop and validate a reproducible and noninvasive test that can accurately grade the severity of liver and vascular disease progression in NAFLD patients.

Recent investigations demonstrated that circulating secreted factors, such as adiponectin, leptin, tumour necrosis factor-α (TNF-α) and fetuin-A significantly affect pathophysiological progression in NAFLD (17–19). Fetuin-A (α2HS-glycoprotein) is a liver glycoprotein secreted into the circulation at high concentrations (20). Fetuin-A is an endogenous inhibitor of insulin receptor tyrosine kinase in the liver and skeletal muscle (21). In mice, a lack of fetuin-A enhances glucose clearance and insulin sensitivity (22). Moreover, Pal *et al.* recently reported that fetuin-A acts as an endogenous ligand for toll-like receptor 4 (TLR4) and enhances both insulin resistance and inflammation (23). These findings suggest that fetuin-A may worsen the course of NAFLD by increasing insulin resistance.

Transforming growth factor-β1 (TGF-β1) is a major pro-fibrogenic growth factor, and enhanced TGF-β1 signalling promotes fibrotic changes in many organs and tissues, including the liver and arteries (24, 25). Fetuin-A is also known to inhibit TGF-β1 signalling (26, 27). The disulphide-looped sequence in the *N*-terminal cystatin domain of fetuin-A shares homology with the extracellular domain of TGF-β receptor type II (TβRII), and this disulphide-looped peptide from fetuin-A binds to TGF-β1 (26). Indeed, fetuin-A knockout mice exhibit worsened organ fibrosis through enhanced TGF-β1 signalling (28, 29). Therefore, the anti-TGF-β1 signalling effects of fetuin-A could prevent organ fibrotic changes, including changes in the liver and vasculature. Thus, fetuin-A seems to promote (e.g. promote insulin resistance) and inhibit (e.g. attenuate organ fibrotic changes) NAFLD progression. However, the significance of serum fetuin-A in liver fibrosis and atherogenic changes in NAFLD subjects remains unknown.

The aim of this study was to elucidate the role of fetuin-A in the progression of liver and vascular fibrosis. To address this issue, we investigated the relationship between the serum fetuin-A level and serum fibrosis markers (platelet count, NAFLD fibrosis score) in NAFLD subjects. We also evaluated the relationship between the serum fetuin-A level and intima media thickness (IMT) and investigated the effects of fetuin-A on hepatic stellate cells (HSCs), which play a pivotal role in the progression of hepatic fibrosis.

Methods

Study subjects

Among 343 Japanese adult subjects (205 males, 138 females) who underwent a health check-up at aMs New Otani Clinic (Osaka, Japan) from 2008 to 2009, 295 subjects (164 males, 131 females) were initially recruited into this study. Exclusion criteria included a history of hepatic disease, such as chronic hepatitis C or concurrent active hepatitis B (seropositive for hepatitis B surface antigen), autoimmune hepatitis, primary biliary cirrhosis, sclerosing cholangitis, haemochromatosis, α1-antitrypsin deficiency, Wilson's disease, or hepatic injury caused by substance abuse, as well as a current or past history of consumption of >20 g of alcohol daily. The diagnosis of fatty liver was based on the results of abdominal ultrasound performed by trained technicians, after exclusion of competing aetiologies of steatogenic liver disease. Fatty liver was defined as liver parenchyma with echogenicity higher than the kidney cortex, the presence of vascular blurring and deep attenuation of the ultrasound signal (30, 31). Of the 295 subjects recruited into this study, 275 (151 males, 124 females) were diagnosed with fatty liver by abdominal ultrasound, whereas 20 subjects (13 males, seven females) were diagnosed as not having fatty liver. Serum samples were collected from the subjects at the time of the health check-up and kept frozen at −80°C until used.

The protocol and informed consent were approved by the institutional review board of the Osaka University Graduate School of Medicine. Written informed consent was obtained from all subjects at the time of health check-up, and this study was conducted in accordance with the Helsinki Declaration.

Anthropometric and laboratory evaluation

Anthropometric variables (height and weight) were measured using a calibrated scale after requesting the patients to remove their shoes and any heavy clothing. Body mass index (BMI) was calculated as weight (kg) divided by the square of height in metres (m^2). Systolic blood pressure (sBP) values were measured in the sitting position to the nearest mm Hg. Venous blood samples were obtained in the morning after overnight fasting for 12 h. Laboratory evaluations for all patients included determination of platelet counts, haemoglobin (Hb), and measurement of serum levels of aspartate aminotransferase (AST), alanine aminotransferase (ALT), γ-glutamyl transpeptidase (GGT), total bilirubin (T-Bil), choline esterase (CHE), creatinine, albumin,

total cholesterol (T-Chol), triglyceride (TG), HDL-cholesterol (HDL-C), fasting blood glucose (FBG), iron and uric acid. All parameters were measured using standard techniques. Impaired fasting glucose (IFG) was defined as a FBG of 110–125 mg/dl. The presence of DM was defined as FBG ≥126 mg/dl, HbA1c (NGSP) ≥6.5% or treatment with antidiabetic drugs. The NAFLD fibrosis score was calculated for each of the subjects as previously reported [1.675 + 0.037 × age (years) + 0.094 × BMI (kg/m^2) + 1.13 × IFG/DM (yes = 1, no = 0) + 0.99 × AST/ALT − 0.013 × platelet count (×10^9/L) − 0.66 × albumin (g/dl)] (32).

IMT measurements

A B-mode examination of the carotid artery was performed using an ultrasound scanner (SSA-660A, Xario; Toshiba Medical Systems Corporation, Tochigi, Japan). The maximum carotid IMT (max IMT) and mean IMT of the common carotid artery were measured on both the right and left sides in the areas of the common carotid artery, bulbus and internal carotid artery (but not the external carotid artery) in the supine position with a 7.5-MHz transducer. The mean IMT was the average thickness of the max IMT at two adjacent points (33).

Enzyme-linked immunosorbent assay (ELISA) for fetuin-A, fucosylated haptoglobin and adiponectin

Fetuin-A levels were determined using a competitive ELISA system, which was established using polyclonal antihuman fetuin antibodies as described previously (34). Briefly, a human fetuin polyclonal antibody was coated as the solid phase (96-well plate), and diluted serum samples were then added to the ELISA plate.

Fucosylated haptoglobin (Fuc-Hpt) levels were measured using our lectin antibody ELISA developed as described previously (35). Briefly, the Fab fragment of antihuman haptoglobin IgG (Dako, Carpinteria, CA) was coated onto the bottom of the wells of a 96-well ELISA plate because IgG has a fucosylated oligosaccharide in its Fc portion. Diluted serum samples were then added to the ELISA plate. To detect Fuc-Hpt, biotinylated *Aleuria aurantia* lectin at a 1/1000 dilution was placed into each well. Adiponectin was measured using a sandwich ELISA system according to the manufacturer's protocol (Otsuka Pharmaceutical Co., Tokushima, Japan) (36). Each assay was performed in duplicate using diluted serum samples.

In vitro assay

The human HSC line LX-2 was kindly donated by Scott Friedman (Mount Sinai School of Medicine) (37). Cells were maintained at 37°C under 5% CO_2 in Dulbecco's modified Eagle's medium (DMEM) containing 10% foetal bovine serum (FBS). LX-2 cells (1.5 × 10^5/well) were seeded in 24-well plates, rested for 24 h, then incubated in serum-free DMEM for 48 h. Cells were stimulated with fetuin-A (15 μM) (Sigma-Aldrich, St-Louis, MO, USA), TGF-β1 (5 ng/ml) (PeproTech EC Ltd., Rocky Hill, CT) or TGF-β1 (5 ng/ml) + fetuin-A (15 μM) dissolved in serum-free DMEM. After 6 h of stimulation, total RNA was extracted from the cells with QIAshredder and an RNeasy Mini Kit according to the manufacturer's instructions (Qiagen, Hilden, Germany) and then transcribed into complementary DNA using a ReverTra Ace qPCR RT Kit (Toyobo, Osaka, Japan). Quantitative real-time reverse transcription polymerase chain reaction (RT-PCR) was performed using the THUNDERBIRD SYBR qPCR Mix (Toyobo, Osaka, Japan) with specific primers on a LightCycler according to the manufacturer's instructions (Roche Diagnostics, Indianapolis, IN, USA). The primers used were TGF-β1 (QT00000728), collagen Iα1 (QT00037793), bone morphogenic protein and activin membrane-bound inhibitor (BAMBI; QT00091329) and glyceraldehyde 3-phosphate dehydrogenase (GAPDH; QT01192646) (Qiagen). mRNA expression levels were normalized to GAPDH mRNA expression and expressed in arbitrary units.

Immunoblot analysis was performed to investigate the phosphorylation of Smad3 (p-Smad3) in LX-2 cells. LX-2 cells (5 × 10^5/well) were seeded in 6-well plates, rested for 24 h, then incubated in serum-free DMEM for 24 h. Cells were stimulated with TGF-β1 (5 ng/ml) with or without fetuin-A (15 μM) for 30 min. Immunoblotting was performed as described previously using rabbit anti-p-Smad3 antibody, anti-Smad3 antibody (Cell Signaling Technology, Beverly, MA, USA) or rabbit anti-GAPDH antibody (Trevigen, Gaithersburg, MD, USA) (38).

Statistical analysis

Statistical analyses were conducted using JMP Pro 10.0 software (SAS Institute Inc., Cary, NC, USA). Continuous variables were expressed as the mean ± standard deviation (SD). Qualitative data were represented as numbers, with percentages indicated in parentheses. Kruskal–Wallis and Wilcoxon tests were used to assess any significant differences in continuous clinical or serological characteristics between groups. Chi-square tests were used for categorical factors. As TG, HDL-C, AST, ALT, GGT and FBG did not show a Gaussian distribution, these parameters were common log transformed before analysis. Spearman's correlation coefficient was used to estimate the association between serum fetuin-A and several factors of interest. The prediction performance of the serum fetuin-A level for increased mean IMT (≥1 mm) was assessed by analyzing receiver operating characteristic (ROC) curves. The probabilities of true positive (sensitivity) and true negative (specificity) assessments, the positive predictive value (PPV) and the negative predictive value (NPV) were determined for selected cut-off values, and the area under the receiver

operating characteristic curve (AUROC) was calculated for each index. The Youden index was used to identify the optimal cut-off value. Univariate and/or multivariate logistic regression analyses were conducted to identify parameters that significantly contribute to platelet count, NAFLD fibrosis score or mean IMT. Differences were considered statistically significant at $P < 0.05$.

Results

Characteristics of the subjects

The clinical and biochemical characteristics of individuals who participated in this study are shown in Table 1. On average, there was no difference in gender between subjects with and without fatty liver. Age was lower and BMI was higher in fatty liver subjects compared with subjects without fatty liver. Serum levels of T-Bil, CHE, TG, FBG, albumin and Hb were also higher in fatty liver subjects. In contrast, ALT, AST/ALT ratio, HDL-C and adiponectin were lower in fatty liver subjects. The max and mean IMT were somewhat lower in fatty liver subjects. This finding conflicted with previous reports indicating that IMT values are higher in NAFLD patients than in normal subjects (39). Age is an independent determinant of the IMT value (40, 41); therefore, the lower IMT in fatty liver patients in this study could be related to their lower age compared with subjects without fatty liver. There were no differences in platelet count or NAFLD fibrosis score between subjects with fatty liver and those without. These data indicate that the fatty liver subjects in our study did not have progressive vascular and liver fibrosis.

The serum Fuc-Hpt level was measured as a noninvasive biomarker for NASH diagnosis (42). Although there was no significant difference in Fuc-Hpt between the two groups, the mean Fuc-Hpt value was higher in subjects without fatty liver, indicating that our control subjects (those without fatty liver) were not completely healthy individuals. Serum fetuin-A levels were higher in fatty liver subjects than in those without fatty liver, but the difference was not significant.

Table 1. Clinical and serological characteristics of the subjects

Factor	All subjects (n = 295)	Without fatty liver (n = 20)	With fatty liver (n = 275)	P* value
Age (y)	56.7 ± 7.0	61.0 ± 7.0	56.4 ± 6.9	<0.01
Gender (M/F)	164/131	13/7	151/124	0.38
BMI (kg/m^2)	26.2 ± 3.7	22.2 ± 2.6	26.5 ± 3.6	<0.01
sBP level (mmHg)	120.7 ± 15.2	117.3 ± 15.5	121.0 ± 15.2	0.34
AST (U/L)	33.3 ± 23.1	35.3 ± 26.5	33.2 ± 22.8	0.63
ALT (U/L)	46.2 ± 36.1	52.1 ± 99.2	45.8 ± 26.6	<0.01
AST/ALT ratio	0.82 ± 0.31	1.08 ± 0.50	0.80 ± 0.28	<0.01
GGT (U/L)	69.3 ± 101.1	114.7 ± 189.1	66.0 ± 91.2	0.66
T-Bil (mg/dl)	0.76 ± 0.30	0.63 ± 0.17	0.77 ± 0.31	<0.05
CHE (IU/L)	390.8 ± 69.0	347.9 ± 87.7	394.0 ± 66.4	<0.01
T-Chol (mg/dl)	212.5 ± 35.3	207.1 ± 43.2	212.9 ± 34.7	0.35
TG (mg/dl)	153.6 ± 97.3	114.1 ± 87.5	156.5 ± 97.4	<0.01
HDL-C (mg/dl)	54.3 ± 11.1	63.4 ± 17.0	53.6 ± 10.3	<0.01
Creatinine (mg/dl)	0.78 ± 0.19	0.84 ± 0.30	0.77 ± 0.18	0.34
FBG (mg/dl)	121.9 ± 33.5	107.5 ± 16.2	123.0 ± 34.2	<0.05
HbA1c (NGSP) (%)	6.78 ± 1.29	6.2 ± 0.7	6.8 ± 1.3	0.10
Albumin (g/dl)	4.4 ± 0.2	4.2 ± 0.2	4.4 ± 0.2	<0.05
Iron (μg/dl)	112.3 ± 38.0	99.2 ± 40.1	113.4 ± 37.8	0.066
Uric acid (mg/dl)	5.8 ± 1.3	5.5 ± 1.1	5.9 ± 1.3	0.16
Hb (g/dl)	14.3 ± 1.2	13.6 ± 1.1	14.3 ± 1.2	<0.01
Platelet count (×10^9/L)	224.1 ± 54.0	212.0 ± 48.7	225.0 ± 54.3	0.29
NAFLD fibrosis score	-1.37 ± 1.10	-1.21 ± 1.01	-1.38 ± 1.10	0.58
Max IMT (mm)	0.93 ± 0.32	1.31 ± 053	0.91 ± 0.29	<0.01
Mean IMT (mm)	0.85 ± 0.24	1.14 ± 0.41	0.83 ± 0.22	<0.01
Adiponectin (μg/ml)	5.11 ± 2.81	8.12 ± 2.77	4.89 ± 2.69	<0.01
Fuc-Hpt (U/ml)	636.0 ± 1065.1	847.4 ± 927.3	620.2 ± 1074.7	0.22
Fetuin-A (μg/ml)	194.9 ± 32.3	182.9 ± 23.6	195.8 ± 32.7	0.074

Data are presented as the mean ± SD.

ALT, alanine aminotransferase; AST, aspartate aminotransferase; BMI, body mass index; CHE, choline esterase; FBG, fasting blood glucose; Fuc-Hpt, fucosylated haptoglobin; GGT, gamma glutamyltranspeptidase; Hb, haemoglobin; IMT, intima media thickness; NAFLD, nonalcoholic fatty liver disease; sBP, systolic blood pressure; T-Bil, total bilirubin; T-Chol, total cholesterol; TG, triglyceride.

*P values correspond to the comparison between without and with fatty liver groups. Wilcoxon test for continuous factors and Pearson's Chi-square test for categorical factors were used.

Relationship between serum fetuin-A, anthropometric parameters and laboratory tests

The results of analyses of Pearson's correlations between serum fetuin-A level and other parameters are summarized in Table 2 and Fig. 1. Serum fetuin-A level was negatively and significantly correlated with age, NAFLD fibrosis score, max IMT and mean IMT. In addition, the serum fetuin-A level was positively and significantly correlated with AST, ALT, GGT and platelet count. The positive correlation between fetuin-A and liver enzymes (AST, ALT and GGT) indicates that fetuin-A promotes liver inflammation. The negative correlation between fetuin-A and NAFLD fibrosis score and the positive correlation between fetuin-A and platelet count indicates that fetuin-A inhibits liver fibrosis. Moreover, the negative correlation between fetuin-A and IMT values indicates that fetuin-A contributes negatively to vascular fibrosis in NAFLD patients.

Relationship between platelet count, anthropometric parameters and laboratory tests

Because advanced liver fibrosis causes portal hypertension and spleen enlargement, thrombocytopaenia has long been known to be accompanied by a degree of liver fibrosis (43–46). We investigated the relationship between platelet count, anthropometric parameters and laboratory tests in NAFLD subjects (Table 3). Univariate analyses revealed that age, AST/ALT ratio, T-Bil, creatinine, iron, Hb and NAFLD fibrosis score had negative relationships, whereas CHE, T-Chol and fetuin-A had positive relationships with the platelet count. We performed multiple logistic regression analyses to determine which variables are significant determinants of the platelet count. Because the platelet count is included in the NAFLD fibrosis score calculation, we omitted the NAFLD fibrosis score from the multiple logistic regression analyses, which demonstrated that age ($P < 0.05$), creatinine ($P < 0.05$), Hb ($P < 0.05$) and serum fetuin-A ($P < 0.05$) levels are significant and independent determinants of the platelet count. Unfortunately, as no spleen diameter data were acquired in our subjects, we could not investigate the relationship between serum fetuin-A and spleen size.

Table 2. Correlation coefficients of relationships between serum fetuin-A levels and various parameters

Factor	*R*	*P* value
Age (y)	−0.21	<0.01
BMI (kg/m^2)	0.17	<0.01
sBP level (mmHg)	0.10	0.084
AST (U/L)	0.23	<0.01
ALT (U/L)	0.27	<0.01
AST/ALT ratio	−0.23	<0.01
GGT (U/L)	0.19	<0.01
T-Bil (mg/dl)	0.031	0.59
CHE (IU/L)	0.19	<0.01
T-Chol (mg/dl)	0.067	0.25
TG (mg/dl)	0.12	<0.05
HDL-C (mg/dl)	−0.027	0.65
Creatinine (mg/dl)	−0.025	0.67
FBG (mg/dl)	−0.012	0.84
HbA1c (NGSP) (%)	−0.071	0.22
Albumin (g/dl)	0.20	<0.01
Iron (μg/dl)	0.18	<0.01
Uric acid (mg/dl)	0.095	0.10
Hb (g/dl)	0.14	<0.05
Platelet count (×10^9/L)	0.19	<0.01
NAFLD fibrosis score	−0.25	<0.01
Max IMT	−0.22	<0.01
Mean IMT	−0.22	<0.01
Adiponectin	−0.11	0.067
Fuc-Hpt	0.058	0.33

Relationship between NAFLD fibrosis score, anthropometric parameters and laboratory tests

The NAFLD fibrosis score is widely used in the noninvasive scoring system to predict the degree of liver fibrosis in NAFLD patients (32). We investigated the relationship between the NAFLD fibrosis score, anthropometric parameters and laboratory tests in NAFLD subjects (Table 4). In univariate analyses, the NAFLD fibrosis score had negative relationships with AST, ALT, GGT, CHE, T-Chol, albumin, platelet count and fetuin-A and positive relationships with age, BMI, AST/ALT ratio, FBG, HbA1c (NGSP) and adiponectin. We omitted age, BMI, AST, ALT, platelet count and albumin from the multiple logistic regression analyses because these variables are considered in the calculation of the NAFLD fibrosis score. The multiple logistic regression analyses demonstrated that T-Chol ($P < 0.01$), adiponectin ($P < 0.05$) and serum fetuin-A levels ($P < 0.01$) were significant and independent determinants of the NAFLD fibrosis score.

Relationship between mean IMT, anthropometric parameters and laboratory tests

Next, we analysed the correlation between the serum fetuin-A level and mean IMT in four groups segmented by mean IMT value quartile (range of mean IMT; group 1: <0.7 mm, group 2: 0.7–0.8 mm, group 3: 0.8–1.0 and group 4: ≥1 mm). Interestingly, the serum fetuin-A level did not change in the three normal mean IMT groups (mean IMT <1 mm) (group 1: 202.3 ± 35.0, group 2: 201.3 ± 31.1 and group 3: 204.0 ± 30.5 μg/ml) but decreased significantly in group 4 (mean IMT ≥1 mm) (180.9 ± 30.1 μg/ml) (Fig. 2A). The AUROC, sensitivity, specificity, PPV and NPV for the prediction of increased mean IMT (≥1 mm) were 0.713%, 66.7%, 74.3%, 46.2%, and 87.1% respectively (Fig. 2B). The serum fetuin-A cut-off value was 183.0 μg/ml.

In addition, we investigated the relationships between mean IMT, anthropometric parameters and

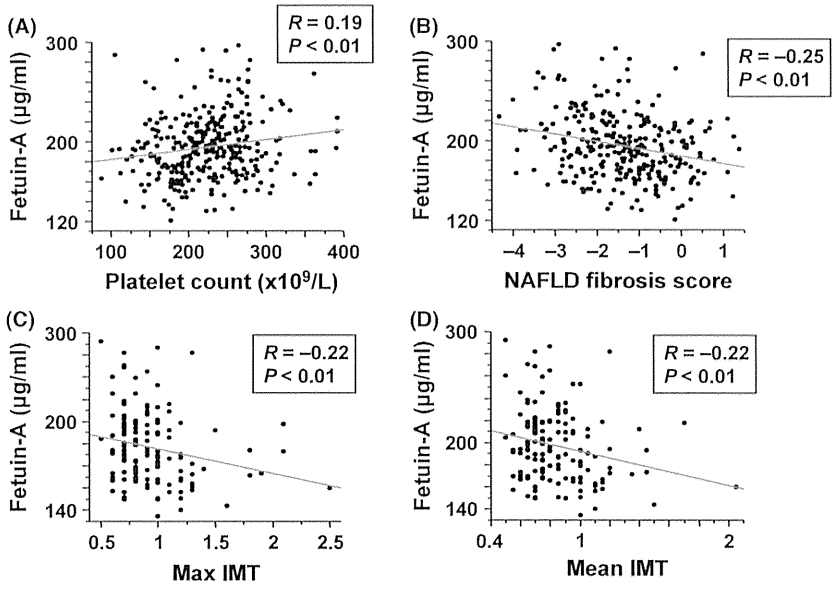

Fig. 1. Relationships between serum fetuin-A level and fibrosis-related factors. Fetuin-A and (A) platelet count, (B) NAFLD fibrosis score, (C) max IMT and (D) mean IMT. R represents the Spearman's correlation coefficient value. NAFLD, nonalcoholic fatty liver disease; IMT, intima media thickness.

Table 3. Univariate and multivariate analysis between platelet count and clinical variables

				95% CI		
Factor	*R*	*P* value	β	Lower	Upper	*P* value
Age (y)	−0.18	<0.01	−1.01	−1.91	−0.11	<0.05
BMI (kg/m^2)	0.10	0.077				
sBP level (mmHg)	−0.0047	0.94				
AST (U/L)	−0.10	0.10				
ALT (U/L)	0.0029	0.96				
AST/ALT ratio	−0.15	<0.05	−18.79	−39.07	1.48	0.069
GGT (U/L)	−0.027	0.65				
T-Bil (mg/dl)	−0.18	<0.01	−13.95	−35.56	7.66	0.20
CHE (IU/L)	0.25	<0.01	0.085	−0.012	0.18	0.086
T-Chol (mg/dl)	0.24	<0.01	0.16	−0.014	0.33	0.072
TG (mg/dl)	−0.085	0.88				
HDL-C (mg/dl)	0.081	0.17				
Creatinine (mg/dl)	−0.24	<0.01	−38.77	−73.39	−4.15	<0.05
FBG (mg/dl)	0.025	0.67				
HbA1c (NGSP) (%)	0.092	0.12				
Albumin (g/dl)	0.045	0.46				
Iron (μg/dl)	−0.13	<0.05	−0.055	−0.23	0.12	0.54
Uric acid (mg/dl)	−0.059	0.31				
Hb (g/dl)	−0.15	<0.05	−7.12	−13.22	−1.02	<0.05
NAFLD fibrosis score	−0.62	<0.01				
Adiponectin (μg/ml)	0.0029	0.96				
Fuc-Hpt (U/ml)	−0.11	0.067				
Fetuin-A (μg/ml)	0.19	<0.01	0.20	0.019	0.39	<0.05

laboratory tests using multiple logistic regression analysis (Table 5). Among the various parameters examined, only the ALT ($P < 0.05$), AST/ALT ratio ($P < 0.01$) and fetuin-A level ($P < 0.05$) were significant and independent determinants of the mean IMT value. We also analysed the relationships between max IMT and other parameters. Multivariate analyses showed that only the AST/ALT ratio was a significant determinant of the max IMT value ($P < 0.05$; data not shown).

Table 4. Univariate and multivariate analysis between NAFLD fibrosis score and clinical variables

Factor	*R*	*P* value	β	95% CI		*P* value
				Lower	Upper	
Age (y)	0.43	<0.01				
BMI (kg/m^2)	0.14	<0.05				
sBP level (mmHg)	0.092	0.13				
AST (U/L)	−0.22	<0.01				
ALT (U/L)	−0.39	<0.01				
AST/ALT ratio	0.45	<0.01				
GGT (U/L)	−0.29	<0.01	−0.00067	−0.0021	0.00081	0.37
T-Bil (mg/dl)	0.024	0.70				
CHE (IU/L)	−0.16	<0.01	−0.0013	−0.0033	0.00074	0.21
T-Chol (mg/dl)	−0.23	<0.01	−0.0059	−0.0096	−0.0022	<0.01
TG (mg/dl)	−0.027	0.66				
HDL-C (mg/dl)	−0.055	0.076				
Creatinine (mg/dl)	0.034	0.58				
FBG (mg/dl)	0.41	<0.01				
HbA1c (NGSP) (%)	0.45	<0.01				
Albumin (g/dl)	−0.33	<0.01				
Iron (μg/dl)	−0.031	0.62				
Uric acid (mg/dl)	−0.066	0.28				
Hb (g/dl)	−0.055	0.37				
Platelet count (×10^9/L)	−0.62	<0.01				
Adiponectin (μg/ml)	0.18	<0.01	0.058	0.014	0.10	<0.05
Fuc-Hpt (U/ml)	0.11	0.074				
Fetuin-A (μg/ml)	−0.25	<0.01	−0.0065	−0.011	−0.0025	<0.01

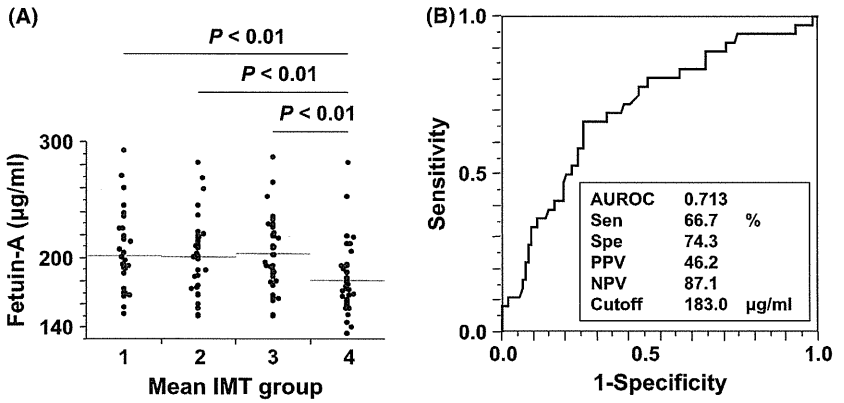

Fig. 2. Serum fetuin-A level in each group, segmented by mean IMT values. Subjects were divided into four groups by quartile of mean IMT value (values of mean IMT; group 1: <0.7 mm, group 2: 0.7–0.8 mm, group 3: 0.8–1.0 and group 4: ≥1 mm). Horizontal grey lines indicate the mean IMT value in each group. ROC curves for fetuin-A for the prediction of increased mean IMT (≥1 mm). AUROC, area under the receiver operating characteristic curve; Sen, sensitivity; Spe, specificity; PPV, positive predictive value; NPV, negative predictive value.

Effects of fetuin-A and TGF-β1 on human hepatic stellate cells

HSCs play a central role in the progression of liver fibrosis (47), and TGF-β1 is the major growth factor involved in liver fibrosis (48). We investigated the effects of human fetuin-A on the HSC line LX-2 with or without TGF-β1 stimulation. We treated LX-2 cells with fetuin-A (15 μM), TGF-β1 (5 ng/ml) or TGF-β1 (5 ng/ml) + fetuin-A (15 μM) and examined fibrosis-related gene expression changes by quantitative real-time RT-PCR (Fig. 3A–C). Treatment of cells with TGF-β1 significantly increased TGF-β1 and collagen Iα1 expression. Treatment with a combination of TGF-β1 and fetuin-A resulted in significant decreases in TGF-β1 and collagen Iα1 levels compared to treatment with TGF-β1 alone. Fetuin-A alone had no significant effect on TGF-β1 and collagen Iα1 gene expression. Interestingly, fetuin-A and TGF-β1 independently upregulated the expression of the TGF-β pseudoreceptor BAMBI, and

Table 5. Multiple logistic regression analysis between mean IMT and clinical variables

Factor	β	95% CI		*P* value
		Lower	Upper	
Age (y)	0.0066	−0.00072	0.014	0.076
BMI (kg/m^2)	−0.0025	−0.020	0.015	0.78
sBP level (mmHg)	0.0017	−0.0015	0.0050	0.30
AST (U/L)	−0.010	−0.021	0.00089	0.071
ALT (U/L)	0.0080	0.00082	0.015	<0.05
AST/ALT ratio	0.56	0.16	0.95	<0.01
GGT (U/L)	−0.00056	−0.0014	0.00026	0.18
T-Bil (mg/dl)	0.050	−0.14	0.24	0.60
CHE (IU/L)	−0.00038	−0.0012	0.00047	0.37
T-Chol (mg/dl)	−0.00052	−0.0023	0.0012	0.56
TG (mg/dl)	−0.00022	−0.00099	0.00055	0.57
HDL-C (mg/dl)	−0.0021	−0.0081	0.0040	0.50
Creatinine (mg/dl)	0.0024	−0.35	0.35	0.99
FBG (mg/dl)	−0.000044	−0.0031	0.0030	0.98
HbA1c (NGSP) (%)	0.0049	−0.070	0.080	0.90
Albumin (g/dl)	−0.0017	−0.26	0.22	0.89
Iron (μg/dl)	−0.000041	−0.0014	0.0013	0.95
Uric acid (mg/dl)	0.0041	−0.038	0.047	0.85
Hb (g/dl)	0.0067	−0.045	0.058	0.80
Platelet count (×10^9/L)	−0.00014	−0.0011	0.00077	0.76
Adiponectin (μg/ml)	−0.0057	−0.025	0.014	0.57
Fuc-Hpt (U/ml)	0.000021	−0.000028	0.000069	0.40
Fetuin-A (μg/ml)	−0.030	−0.055	−0.0084	<0.05

costimulation with fetuin-A and TGF-β1 further upregulated BAMBI expression in LX-2 cells.

Next, we examined the phosphorylation of Smad3 after TGF-β1 stimulation with or without fetuin-A (Fig. 3D). We found that fetuin-A attenuated TGF-β1-induced phosphorylation of Smad3. These data indicate that fetuin-A could suppress TGF-β1 signalling.

Discussion

Our present study involving subjects who received medical health check-ups demonstrated that the serum fetuin-A level is significantly and negatively correlated with both liver and vascular fibrosis in NAFLD. Multivariate analyses revealed that the serum fetuin-A level is an independent determinant of platelet count, NAFLD fibrosis score and mean IMT. In addition, our *in vitro* study demonstrated that fetuin-A blocks TGF-β1-induced fibrogenic signalling. The results of both our human and *in vitro* studies were consistent and indicate that measurement of the serum fetuin-A level is useful for predicting liver and vascular fibrotic changes in NAFLD subjects.

A recent cross-sectional multicenter study reported that type 2 DM affects the severity of liver fibrosis in NAFLD patients (49). In addition, the presence of type 2 DM is an independent risk factor for atherosclerotic diseases (50). In the present study, we demonstrated that the serum fetuin-A concentration decreases with the progression of liver and vascular fibrosis in NAFLD patients (Figs 1 and 2). Decreased serum fetuin-A levels and insulin resistance in NAFLD patients should synergistically accelerate the progression of both liver and vascular fibrogenesis.

NAFLD is a rapidly growing worldwide medical problem because of the ongoing epidemics of obesity and type 2 DM (51). The prevalence of NAFLD in the general population ranges from 15% to 39% (4, 52), and approximately 30% of Japanese adults have NAFLD (5). Recently, Kahraman *et al.* reported that the serum fetuin-A level is significantly higher in NASH patients than in simple steatosis patients (53). Because fetuin-A is a pro-inflammatory protein secreted by hepatocytes, the inflammation in NASH-affected liver would enhance hepatic fetuin-A production. Interestingly, Ballestri *et al.* reported that the serum fetuin-A level is significantly lower in NAFLD patients with CVD than in NAFLD patients without CVD (54). In addition, they found that elevated serum fetuin-A levels are an independent negative predictor of CVD. Their findings were consistent with ours. Both their study and ours indicate that elevated serum fetuin-A levels in NAFLD patients prevent liver and vascular fibrosis as a self-defence reaction (Fig. 4).

In this study, we showed that fetuin-A inhibits TGF-β signalling in LX-2 HSCs, a result which is in agreement with previous reports (27, 55). Interestingly, our study demonstrated that fetuin-A upregulates BAMBI expression. BAMBI is a TGF-β pseudoreceptor and part of a major negative TGF-β signalling feedback mechanism in HSCs (56, 57). To investigate this major negative feedback pathway in HSCs in the presence and absence of fetuin-A, we analysed the expression of BAMBI. However, the mechanism through which fetuin-A upregulates BAMBI remains unknown. Further investigations are needed to elucidate the precise mechanism.

Our study has some limitations. Firstly, the diagnosis of NAFLD was made by ultrasound, and not all subjects received a liver biopsy. Therefore, we could not investigate the relationship between serum fetuin-A levels and the degree of liver fibrosis. In addition, we could not quantitatively estimate liver fat deposition using ultrasonography. Because our study subjects were recruited from health check-ups, liver biopsy was not feasible for all of the subjects because of ethical concerns. In the near future, we will investigate this relationship in biopsy-proven NAFLD patients who were clinically indicated for liver biopsy. Secondly, we did not measure serum fasting insulin levels in our subjects and could not evaluate the precise degree of insulin resistance. We

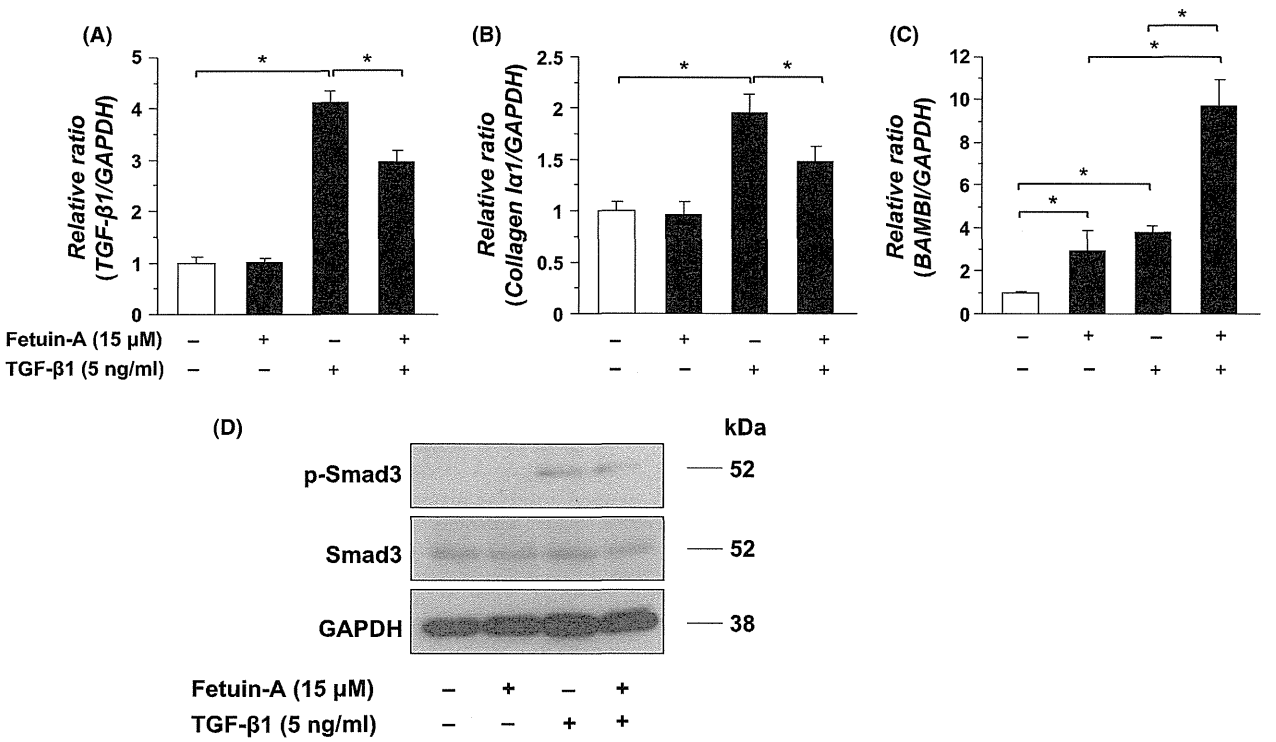

Fig. 3. The effects of fetuin-A and TGF-β1 on human LX-2 HSCs. Levels of (A) TGF-β1, (B) collagen Iα1 and (C) BAMBI gene expression in LX-2 cells with (+) or without (−) fetuin-A (15 μM) and TGF-β1 (5 ng/ml). Levels of gene expression were normalized to GAPDH gene expression and expressed in arbitrary units. Data are means ± SD. *$P < 0.05$ (Wilcoxon test). BAMBI, bone morphogenic protein and activin membrane-bound inhibitor. (D) Immunoblot analysis of p-Smad3, Smad3 and GAPDH. LX-2 cells were incubated for 30 min with (+) or without (−) fetuin-A (15 μM) and TGF-β1 (5 ng/ml). A total of 15 μg of LX-2 whole-cell lysate protein was applied for immunoblotting analysis.

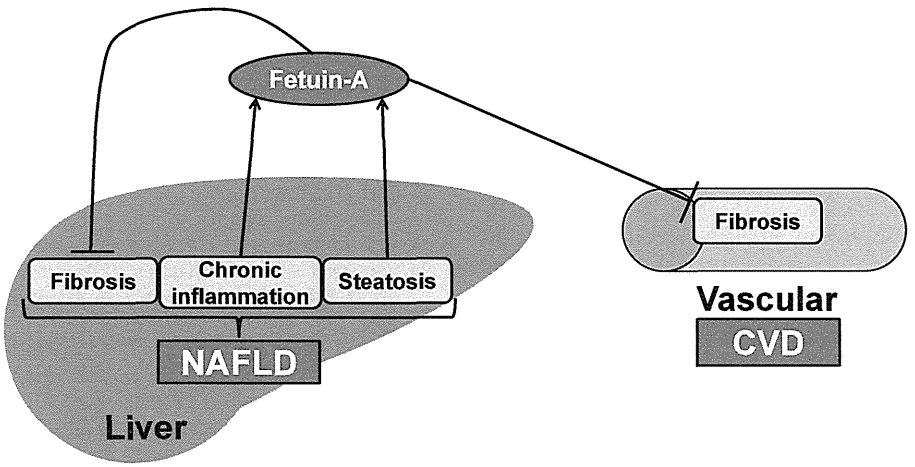

Fig. 4. Putative relationships linking NAFLD, fetuin-A and CVD. We propose that the level of fetuin-A, which increases with chronic inflammatory and fatty changes in the liver, directly suppresses the progression of both liver and vascular fibrosis. CVD, cardiovascular disease.

measured FBG but found no significant relationship between the serum fetuin-A level and FBG. Thirdly, the number of subjects with severe IMT in our study was insufficient to examine the relationship between the serum fetuin-A level and mean IMT precisely in the subjects with vascular fibrosis. Although there was no significant change in the serum fetuin-A level in subjects with normal mean IMT (<1 mm), the level decreased significantly in subjects with abnormal mean IMT (≥1 mm). These results indicate that a decrease in serum fetuin-A level may be a good predictor of the onset of early atherosclerosis. Finally, our study did not

prospectively assess the diagnostic value of fetuin-A in a validation cohort, but we plan to do so in a future study.

In conclusion, measurement of the level of fetuin-A is a noninvasive method, and our results indicate that fetuin-A might prove to be a useful biomarker for predicting liver and vascular fibrosis in NAFLD patients who received health check-ups. Low serum fetuin-A levels are suggestive of enhanced progression of liver and vascular fibrosis in NAFLD patients.

Acknowledgements

The authors would like to thank Akiko Shirai (Research & Development Div., DS Pharma Biomedical Co., Ltd.) for development and technical assistance with the fetuin ELISA kit.

Financial support: This study was supported by Grants-in-Aid for Scientific Research (A), No. 21249038, and (C), No. 24590972, from the Japan Society for the Promotion of Science and by the Global COE Program of Osaka University, funded by the Ministry of Education, Culture, Sports, Science, and Technology of Japan.

Conflicts of interests: The authors do not have any disclosures to report.

References

1. Ford ES, Giles WH, Dietz WH. Prevalence of the metabolic syndrome among US adults: findings from the third National Health and Nutrition Examination Survey. *JAMA* 2002; **287**: 356–9.
2. Bugianesi E, Leone N, Vanni E, *et al.* Expanding the natural history of nonalcoholic steatohepatitis: from cryptogenic cirrhosis to hepatocellular carcinoma. *Gastroenterology* 2002; **123**: 134–40.
3. Neuschwander-Tetri BA, Caldwell SH. Nonalcoholic steatohepatitis: summary of an AASLD Single Topic Conference. *Hepatology* 2003; **37**: 1202–19.
4. Browning JD, Szczepaniak LS, Dobbins R, *et al.* Prevalence of hepatic steatosis in an urban population in the United States: impact of ethnicity. *Hepatology* 2004; **40**: 1387–95.
5. Eguchi Y, Hyogo H, Ono M, *et al.* Prevalence and associated metabolic factors of nonalcoholic fatty liver disease in the general population from 2009 to 2010 in Japan: a multicenter large retrospective study. *J Gastroenterol* 2012; **47**: 586–95.
6. Angulo P. Nonalcoholic fatty liver disease. *N Engl J Med* 2002; **346**: 1221–31.
7. Liou I, Kowdley KV. Natural history of nonalcoholic steatohepatitis. *J Clin Gastroenterol* 2006; **40**(Suppl. 1): S11–6.
8. Nascimbeni F, Pais R, Bellentani S, *et al.* From NAFLD in clinical practice to answers from guidelines. *J Hepatol* 2013; **59**: 859–71.
9. Vanni E, Bugianesi E, Kotronen A, *et al.* From the metabolic syndrome to NAFLD or vice versa? *Dig Liver Dis* 2010; **42**: 320–30.
10. Anstee QM, Targher G, Day CP. Progression of NAFLD to diabetes mellitus, cardiovascular disease or cirrhosis. *Nat Rev Gastroenterol Hepatol* 2013; **10**: 330–44.
11. Ou HY, Wang CY, Yang YC, Chen MF, Chang CJ. The association between nonalcoholic fatty pancreas disease and diabetes. *PLoS ONE* 2013; **8**: e62561.
12. Oni ET, Agatston AS, Blaha MJ, *et al.* A systematic review: burden and severity of subclinical cardiovascular disease among those with nonalcoholic fatty liver; should we care? *Atherosclerosis* 2013; **230**: 258–67.
13. Villanova N, Moscatiello S, Ramilli S, *et al.* Endothelial dysfunction and cardiovascular risk profile in nonalcoholic fatty liver disease. *Hepatology* 2005; **42**: 473–80.
14. Salvi P, Ruffini R, Agnoletti D, *et al.* Increased arterial stiffness in nonalcoholic fatty liver disease: the Cardio-GOOSE study. *J Hypertens* 2010; **28**: 1699–707.
15. Targher G, Bertolini L, Padovani R, *et al.* Prevalence of nonalcoholic fatty liver disease and its association with cardiovascular disease among type 2 diabetic patients. *Diabetes Care* 2007; **30**: 1212–8.
16. Lonardo A, Sookoian S, Chonchol M, Loria P, Targher G. Cardiovascular and systemic risk in nonalcoholic fatty liver disease - atherosclerosis as a major player in the natural course of NAFLD. *Curr Pharm Des* 2013; **19**: 5177–92.
17. Kamada Y, Takehara T, Hayashi N. Adipocytokines and liver disease. *J Gastroenterol* 2008; **43**: 811–22.
18. Stefan N, Kantartzis K, Haring HU. Causes and metabolic consequences of Fatty liver. *Endocr Rev* 2008; **29**: 939–60.
19. Tonjes A, Fasshauer M, Kratzsch J, Stumvoll M, Bluher M. Adipokine pattern in subjects with impaired fasting glucose and impaired glucose tolerance in comparison to normal glucose tolerance and diabetes. *PLoS ONE* 2010; **5**: e13911.
20. Denecke B, Graber S, Schafer C, *et al.* Tissue distribution and activity testing suggest a similar but not identical function of fetuin-B and fetuin-A. *Biochem J* 2003; **376**(Pt. 1): 135–45.
21. Srinivas PR, Wagner AS, Reddy LV, *et al.* Serum alpha 2-HS-glycoprotein is an inhibitor of the human insulin receptor at the tyrosine kinase level. *Mol Endocrinol* 1993; **7**: 1445–55.
22. Mathews ST, Singh GP, Ranalletta M, *et al.* Improved insulin sensitivity and resistance to weight gain in mice null for the Ahsg gene. *Diabetes* 2002; **51**: 2450–8.
23. Pal D, Dasgupta S, Kundu R, *et al.* Fetuin-A acts as an endogenous ligand of TLR4 to promote lipid-induced insulin resistance. *Nat Med* 2012; **18**: 1279–85.
24. Gressner AM, Weiskirchen R, Breitkopf K, Dooley S. Roles of TGF-beta in hepatic fibrosis. *Front Biosci* 2002; **7**: d793–807.
25. Toma I, Mccaffrey TA. Transforming growth factor-beta and atherosclerosis: interwoven atherogenic and atheroprotective aspects. *Cell Tissue Res* 2012; **347**: 155–75.
26. Rittenberg B, Partridge E, Baker G, *et al.* Regulation of BMP-induced ectopic bone formation by Ahsg. *J Orthop Res* 2005; **23**: 653–62.
27. Verma-Gandhu M, Peterson MR, Peterson TC. Effect of fetuin, a TGFbeta antagonist and pentoxifylline, a cytokine antagonist on hepatic stellate cell function and fibrotic parameters in fibrosis. *Eur J Pharmacol* 2007; **572**: 220–7.
28. Merx MW, Schafer C, Westenfeld R, *et al.* Myocardial stiffness, cardiac remodeling, and diastolic dysfunction in calcification-prone fetuin-A-deficient mice. *J Am Soc Nephrol* 2005; **16**: 3357–64.
29. Guillory B, Sakwe AM, Saria M, *et al.* Lack of fetuin-A (alpha2-HS-glycoprotein) reduces mammary tumor inci-

dence and prolongs tumor latency via the transforming growth factor-beta signaling pathway in a mouse model of breast cancer. *Am J Pathol* 2010; **177**: 2635–44.
30. Saadeh S, Younossi ZM, Remer EM, *et al.* The utility of radiological imaging in nonalcoholic fatty liver disease. *Gastroenterology* 2002; **123**: 745–50.
31. Hamano M, Kamada Y, Kiso S, *et al.* Adiponectin negatively correlates with alcoholic and non-alcoholic liver dysfunction: health check-up study of Japanese men. *Hepatol Res* 2013; **43**: 238–48.
32. Angulo P, Hui JM, Marchesini G, *et al.* The NAFLD fibrosis score: a noninvasive system that identifies liver fibrosis in patients with NAFLD. *Hepatology* 2007; **45**: 846–54.
33. Hirata A, Kishida K, Hiuge-Shimizu A, *et al.* Qualitative score of systemic arteriosclerosis by vascular ultrasonography as a predictor of coronary artery disease in type 2 diabetes. *Atherosclerosis* 2011; **219**: 623–9.
34. Kuwamoto K, Takeda Y, Shirai A, *et al.* Identification of various types of alpha2-HS glycoprotein in sera of patients with pancreatic cancer: possible implication in resistance to protease treatment. *Mol Med Rep* 2010; **3**: 651–6.
35. Kamada Y, Kinoshita N, Tsuchiya Y, *et al.* Reevaluation of a lectin antibody ELISA kit for measuring fucosylated haptoglobin in various conditions. *Clin Chim Acta* 2013; **417**: 48–53.
36. Kumada M, Kihara S, Sumitsuji S, *et al.* Association of hypoadiponectinemia with coronary artery disease in men. *Arterioscler Thromb Vasc Biol* 2003; **23**: 85–9.
37. Xu L, Hui AY, Albanis E, *et al.* Human hepatic stellate cell lines, LX-1 and LX-2: new tools for analysis of hepatic fibrosis. *Gut* 2005; **54**: 142–51.
38. Kamada Y, Mori K, Matsumoto H, *et al.* N-Acetylglucosaminyltransferase V regulates TGF-beta response in hepatic stellate cells and the progression of steatohepatitis. *Glycobiology* 2012; **22**: 778–87.
39. Sookoian S, Pirola CJ. Non-alcoholic fatty liver disease is strongly associated with carotid atherosclerosis: a systematic review. *J Hepatol* 2008; **49**: 600–7.
40. Aminbakhsh A, Mancini GB. Carotid intima-media thickness measurements: what defines an abnormality? A systematic review. *Clin Invest Med* 1999; **22**: 149–57.
41. Lorenz MW, Markus HS, Bots ML, Rosvall M, Sitzer M. Prediction of clinical cardiovascular events with carotid intima-media thickness: a systematic review and meta-analysis. *Circulation* 2007; **115**: 459–67.
42. Kamada Y, Akita M, Takeda Y, *et al.* Serum Fucosylated Haptoglobin as a Novel Diagnostic Biomarker for Predicting Hepatocyte Ballooning and Nonalcoholic Steatohepatitis. *PLoS ONE* 2013; **8**: e66328.
43. Liaw YF, Tai DI, Chu CM, Chen TJ. The development of cirrhosis in patients with chronic type B hepatitis: a prospective study. *Hepatology* 1988; **8**: 493–6.
44. Poynard T, Yuen MF, Ratziu V, Lai CL. Viral hepatitis C. *Lancet* 2003; **362**: 2095–100.
45. Udell JA, Wang CS, Tinmouth J, *et al.* Does this patient with liver disease have cirrhosis? *JAMA* 2012; **307**: 832–42.
46. Cozzolino G, Lonardo A, Francica G, Amendola F, Cacciatore L. Differential diagnosis between hepatic cirrhosis and chronic active hepatitis: specificity and sensitivity of physical and laboratory findings in a series from the Mediterranean area. *Am J Gastroenterol* 1983; **78**: 442–5.
47. Friedman SL. Seminars in medicine of the Beth Israel Hospital, Boston. The cellular basis of hepatic fibrosis. Mechanisms and treatment strategies. *N Engl J Med* 1993; **328**: 1828–35.
48. Bedossa P, Peltier E, Terris B, Franco D, Poynard T. Transforming growth factor-beta 1 (TGF-beta 1) and TGF-beta 1 receptors in normal, cirrhotic, and neoplastic human livers. *Hepatology* 1995; **21**: 760–6.
49. Nakahara T, Hyogo H, Yoneda M, *et al.* Type 2 diabetes mellitus is associated with the fibrosis severity in patients with nonalcoholic fatty liver disease in a large retrospective cohort of Japanese patients. *J Gastroenterol* 2014. (in press).
50. Milicevic Z, Raz I, Beattie SD, *et al.* Natural history of cardiovascular disease in patients with diabetes: role of hyperglycemia. *Diabetes Care* 2008; **31**(Suppl. 2): S155–60.
51. Charlton M. Nonalcoholic fatty liver disease: a review of current understanding and future impact. *Clin Gastroenterol Hepatol* 2004; **2**: 1048–58.
52. Powell EE, Cooksley WG, Hanson R, *et al.* The natural history of nonalcoholic steatohepatitis: a follow-up study of forty-two patients for up to 21 years. *Hepatology* 1990; **11**: 74–80.
53. Kahraman A, Sowa JP, Schlattjan M, *et al.* Fetuin-A mRNA expression is elevated in NASH compared with NAFL patients. *Clin Sci (Lond)* 2013; **125**: 391–400.
54. Ballestri S, Meschiari E, Baldelli E, *et al.* Relationship of serum fetuin-a levels with coronary atherosclerotic burden and NAFLD in patients undergoing elective coronary angiography. *Metab Syndr Relat Disord* 2013; **11**: 289–95.
55. Demetriou M, Binkert C, Sukhu B, Tenenbaum HC, Dennis JW. Fetuin/alpha2-HS glycoprotein is a transforming growth factor-beta type II receptor mimic and cytokine antagonist. *J Biol Chem.* 1996; **271**: 12755–61.
56. Seki E, De Minicis S, Osterreicher CH, *et al.* TLR4 enhances TGF-beta signaling and hepatic fibrosis. *Nat Med* 2007; **13**: 1324–32.
57. Sekiya T, Oda T, Matsuura K, Akiyama T. Transcriptional regulation of the TGF-beta pseudoreceptor BAMBI by TGF-beta signaling. *Biochem Biophys Res Commun* 2004; **320**: 680–4.

Pancreatic Fatty Degeneration and Fibrosis as Predisposing Factors for the Development of Pancreatic Ductal Adenocarcinoma

Yasuhiko Tomita, MD, PhD, Kanako Azuma, MS,† Yuji Nonaka, MS,† Yoshihiro Kamada, MD, PhD,† Miki Tomoeda, DDS, PhD,* Mioka Kishida, MD,* Masahiro Tanemura, MD, PhD,‡ and Eiji Miyoshi, MD, PhD†*

Objectives: Knowledge of risk factors for development of pancreatic ductal adenocarcinoma (PDAC) is limited. To clarify the background condition of the pancreas for the development of PDAC, we analyzed pancreatic histological changes in noncancerous lesion specimens after pancreatectomy in PDAC patients.

Methods: Seventy-six patients with PDAC were enrolled in this study. The PDAC was in the pancreatic head in 37 patients, in the body in 31, and in the tail in 8. No patients had a history of clinical chronic pancreatitis. As controls, 98 patients without PDAC were enrolled. The following parameters were examined: fibrosis, fatty degeneration, and inflammatory cell infiltration. More than 5% of fatty degeneration in the specimen, more than 10% of fibrosis, and more than 5% of inflammatory cell infiltration were considered positive changes.

Results: Pancreatectomy specimens showed a higher ratio of positive change in fibrosis (86% vs 42%), fatty degeneration (72% vs 44%), and inflammatory cell infiltration (14% vs 3%) than control samples. Multivariate analyses demonstrated that each histological change was a significant, independent determinant for PDAC.

Conclusions: Our study demonstrated that cryptogenic pancreatic inflammation with fatty changes represents an important predisposing factor for PDAC. Screening for subclinical chronic pancreatitis in healthy populations may enable the detection of PDAC at an early stage.

Key Words: chronic pancreatitis (CP), fatty degeneration, fibrosis, inflammatory cell infiltration, alcoholic fatty pancreas disease (AFPD), nonalcoholic fatty pancreas disease (NAFPD)

(*Pancreas* 2014;00: 00–00)

Pancreatic ductal adenocarcinoma (PDAC) is one of the most fatal cancers, showing a high potential for invasive activity, early recurrence, and high recurrence rates.[1–5] Most patients with PDAC are diagnosed at an advanced stage, such as stage III or IV, and the tumors are usually unresectable.[1] Even in resectable cases, the prognosis of patients with PDAC is very poor because of local recurrence or distant metastasis within a short period after the operation.[3–5]

Chronic pancreatitis (CP) has been identified as a strong risk factor for PDAC occurrence.[6–8] It is morphologically defined as progressive pancreatic fibrosis and inflammation that is accompanied by atrophy of pancreatic exocrine cells.[9,10] The main cause of CP is alcohol consumption.[11] Repeated acute pancreatitis induced by alcohol consumption induces CP. Meanwhile, nonalcoholic fatty pancreas disease (NAFPD) was recently recognized as a new clinical entity of obesity-related disease.[12,13] In patients with NAFPD, the level of pancreatic fatty degeneration increases with the degree of obesity, and obesity is known to increase the PDAC mortality rate.[14] However, whether NAFPD can progress to CP and PDAC is currently unclear.

Chronic inflammation is thought to induce fibrosis in the advanced stage. In contrast, fibrosis is commonly observed around cancerous lesions in surgical specimens of PDAC and is considered to be induced by cancer cells.[15–18] One cause of this fibrosis is that pancreatic cancer cells activate the pancreatic stellate cells (PSCs) around them, and this activation leads to fibrosis of the tumor. A second common cause is that PDAC originates from the pancreatic ductal system. The PDAC may obstruct the smaller ductules and even the main duct. The PSCs distal to the lesion are activated because of ductal obstruction, resulting in pancreatitis.[15–18] A third possibility is that PDAC results from chronic inflammation due to pancreatitis in tissue surrounding the PDAC.

Difficulty in the early detection of PDAC is due to the lack of subjective symptoms in most patients with PDAC.[3–5] Therefore, efforts have been made to identify populations at high risk for developing PDAC.[19–26] Individuals with a familial history of PDAC, Peutz-Jeghers syndrome, and germline mutations in *BRCA2*, *PALB2*, *p16*, *STK11*, *ATM*, *PRSS1*, and hereditary colon cancer (Lynch syndrome) genes have been considered to be groups at high risk for PDAC development.[19–26] Moreover, a recent genome-wide association study revealed that people with blood group O have a lower susceptibility to PDAC than people with blood group A or B.[27] In acquired factors, smoking, diabetes, alcohol consumption, central obesity in men, infection with *Helicobacter pylori*, and CP are risk factors for PDAC development.[11,14,28] However, little consensus has been reached about the histological factors that predispose the pancreas to the development of PDAC.

In this study, our hypothesis is that PDAC may develop from subclinical cryptogenic CP. This concept is similar to that of chronic liver diseases, such as induced hepatocellular carcinoma (HCC). In subclinical CP patients, NAFPD and alcoholic fatty pancreas disease (AFPD) may be major causes of PDAC. To investigate this hypothesis, noncancerous regions of

From the *Department of Pathology, Osaka Medical Center for Cancer and Cardiovascular Diseases, Osaka, Japan; †Department of Molecular Biochemistry and Clinical Investigation, Osaka University Graduate School of Medicine, Osaka, Japan; and ‡Department of Surgery, National Hospital Organization Kure Medical Center, Hiroshima, Japan.

Received for publication July 9, 2013; accepted May 23, 2014.

Reprints: Yasuhiko Tomita, MD, PhD, Department of Pathology, Osaka Medical Center for Cancer and Cardiovascular Diseases, 1-3-3 Nakamichi, Higashinari, Osaka 537-8511, Japan (e-mail: yasuhiko-tomita@umin.ac.jp); and Eiji Miyoshi, MD, PhD, Department of Molecular Biochemistry and Clinical Investigation, Osaka University Graduate School of Medicine, 1-7 Yamada-oka, Suita, Osaka 565-0871, Japan (e-mail: emiyoshi@sahs.med.osaka-u.ac.jp).

This study was supported by a Grant-in-Aid for Scientific Research (C) No. 24590459 from the Japan Society for the Promotion of Science.

The authors declare no conflict of interest.

Supplemental digital contents are available for this article. Direct URL citations appear in the printed text and are provided in the HTML and PDF versions of this article on the journal's Web site (www.pancreasjournal.com).

the pancreas that had been surgically resected for PDAC were histologically examined for chronic changes such as fatty degeneration, fibrosis, and infiltration of inflammatory cells. As controls, pancreatic specimens in patients without PDAC obtained at autopsy were used. The primary outcome of our study was the presence of PDAC, and the secondary outcome was the histological changes (fibrosis, fatty degeneration, and inflammatory cell infiltration).

MATERIALS AND METHODS

Patients With PDAC and Control Autopsy Samples

Seventy-six patients who underwent surgical resection for PDAC were selected for the present study. They underwent surgery at the Osaka Medical Center for Cancer and Cardiovascular Diseases from May 2008 to September 2010. This group included 41 male and 35 female patients with a median age of 66 years (range, 35–88 years). T-classification (Union for International Cancer Control's) of our patients was shown in Supplementary Table 1, http://links.lww.com/MPA/A303. The PDAC was located in the pancreatic head in 37 patients, in the body in 31, and in the tail in 8. Forty-two patients (55%) received neoadjuvant chemoradiotherapy (CRT) for PDAC. As controls, pancreas samples were obtained at autopsy from 98 patients (62 male and 36 female patients) without PDAC with a median age of 65 years (range, 22–90 years) at the Osaka Medical Center for Cancer and Cardiovascular Diseases from May 2001 to July 2011.

The chief complaints of the patients with PDAC were abdominal pain/discomfort in 12 patients, diabetes mellitus (DM) in 9, back pain in 7, weight loss/anorexia in 6, jaundice in 3, and no symptoms (including during medical checkups and for the follow-up for other diseases) in 32. Technical procedures for detecting pancreatic cancer were computed tomography in 38 patients, endoscopic retrograde cholangiopancreatography in 22, ultrasound in 21, increase in tumor markers in 11, magnetic resonance imaging in 9, cytological examination in 5, and positron emission tomography in 4.

The histories of the patients with PDAC were as follows: hypertension in 11, colon polyps in 9, appendicitis in 7, duodenal ulcers in 5, prostate cancer and hyperplasia in 4, cholelithiasis in 4, hepatitis in 4, angina pectoris in 3, tuberculosis in 2, and gastric ulcers in 2. Among the 35 female patients, an ovarian cystoma was found in 3 patients, breast cancer was found in 2, and uterine myomas was found in 2.

The causes of death of the patients who underwent autopsy were as follows: lung cancer in 14 patients, hepatoma in 11, gastric cancer in 8, urinary bladder cancer in 6, malignant lymphoma in 6, cervical cancer in 6, liver cirrhosis in 5, sepsis in 5, ovarian cancer in 5, esophageal cancer in 4, breast cancer in 3, osteosarcoma in 3, and leukemia in 3.

Laboratory data including the levels of HbA1c, glucose, amylase, P-amylase, elastase, CA19-9, and DUPAN-2 were also examined. The presence of DM was defined as fasting blood glucose of 126 mg/dL or greater, HbA1c (NGSP) of 6.5% or greater, or treatment with antidiabetic drugs. The Brinkman

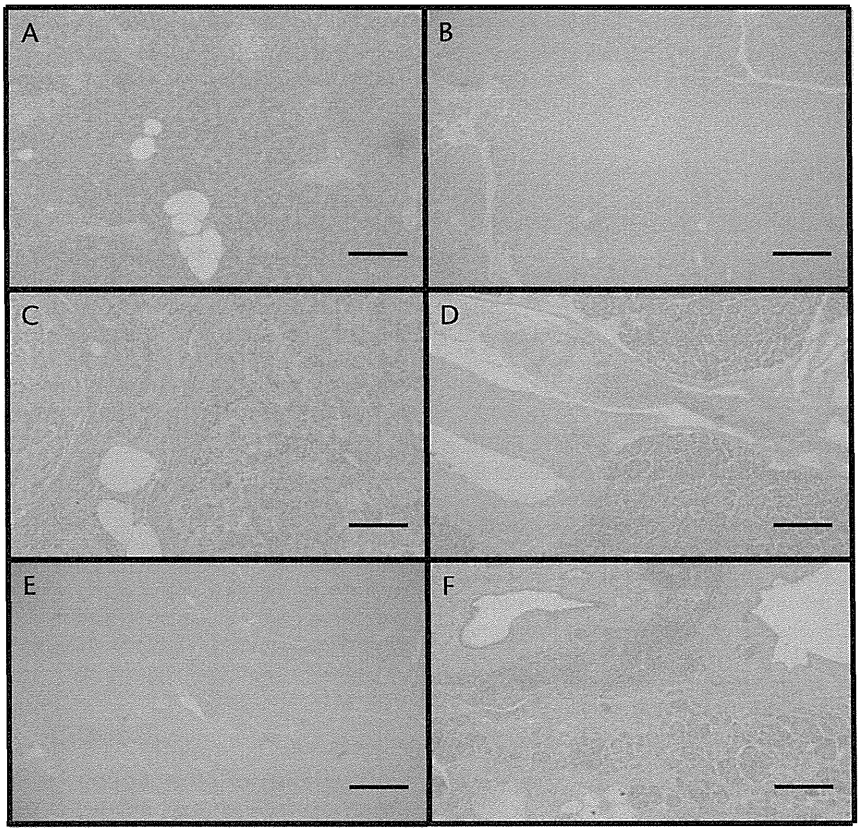

FIGURE 1. Pathological evaluation of lymphocyte infiltration. A and B represent grade 0 or 1 (<5% of lymphocyte infiltration), C and D epresent grade 2 or 3 (6%–15% of [moderate] lymphocyte infiltration), and E and F represent grade 4 (>16% of [severe] lymphocyte infiltration). A, C, and E show the pancreas region of patients with PDAC, and B, D, and F show the pancreas region of non-PDAC patients. In patients with PDAC, severe fibrosis was observed with lymphocyte infiltration. Each scale bar in the figure shows 500 μm.

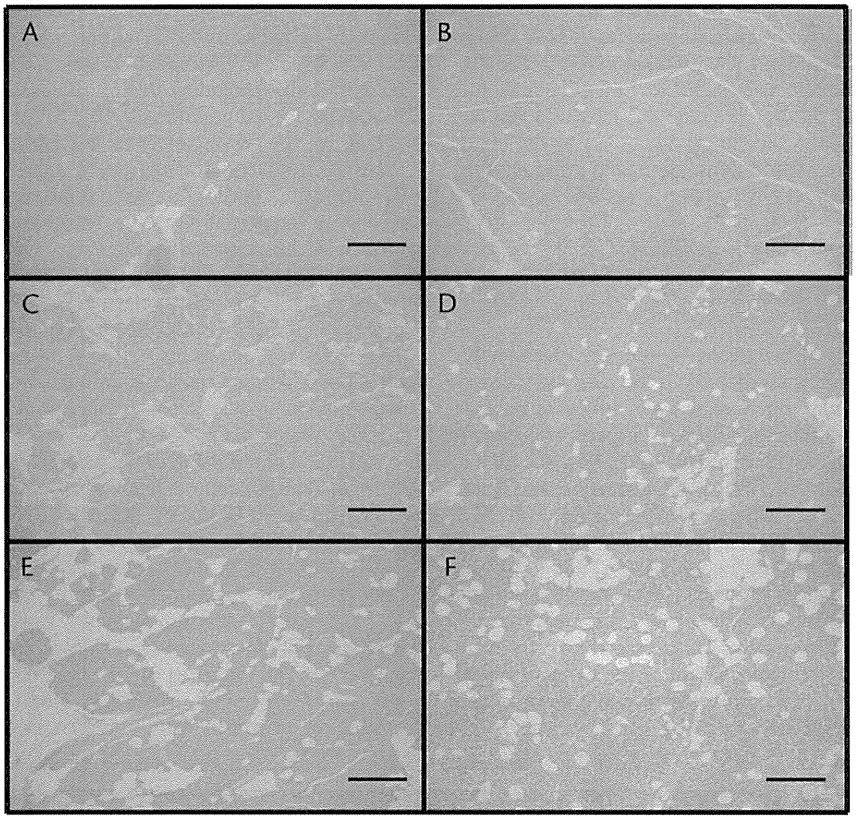

FIGURE 2. Pathological evaluation of fatty degeneration. A and B represent grade 0 or 1 (<5% of fatty change), C and D represent grade 2 or 3 (6%–15% of [moderate] fatty change), and E and F represent grade 4 (>16% of [severe] fatty change). A, C, and E show the pancreas region of patients with PDAC, and B, D, and F show the pancreas region of non-PDAC patients. Each scale bar in the figure shows 500 μm.

index was calculated as the number of cigarettes smoked per day multiplied by the number of years that the participant smoked.[29]

Surgically Resected and Autopsy Specimens of the Pancreas

Surgically resected specimens were fixed in 10% of formalin and cut to 1-cm thickness. All sections were then routinely processed for paraffin embedding. Histological sections cut to 2-μm thickness were stained with hematoxylin and eosin and microscopically examined to determine the extent of PDAC. A section without cancerous lesions was selected to detect the presence of fatty degeneration, fibrosis, and inflammatory cell infiltration. Three authors independently reviewed the extent of fatty degeneration, fibrosis, and infiltration and categorized each lesion into 5 grades as developed by us and ranging from 0 to 4 (Fig. 1). Inflammatory cell infiltration was categorized as grade 0 (no inflammatory cells observed), 1 (1%–5% of inflammatory cells), 2 (6%–10%), 3 (11–15%), or 4 (>16%). Grades 0 and 1 were defined as negative for lymphocyte infiltration, grades 2 and 3 were defined as moderate infiltration of lymphocytes, and grade 4 was defined as severe infiltration of lymphocytes. As shown in Figure 2, fatty degeneration was categorized as grade 0 (0%–1% of fatty change in the pancreas), 1 (2%–5%), 2 (6%–10%), 3 (11%–15%), or 4 (>16%). Grades 0 and 1 were defined as negative for fatty degeneration, grades 2 and 3 were defined as moderate fatty degeneration, and grade 4 was defined as severe fatty degeneration. As shown in Figure 3, fibrosis was categorized as grade 0 (<5% of fibrotic change in the pancreas), 1 (6%–10%), 2 (11%–20%), 3 (21%–30%), or 4 (>31%). Grades 0 and 1 were defined as negative for fibrosis, grades 2 and 3 were defined as moderate fibrosis, and grade 4 was defined as severe fibrosis. For each parameter, grades 0 and 1 were reassessed as negative, and grades 2 to 4 were reassessed as positive. The Kappa values for the scores (fatty degeneration, inflammatory cell infiltration, and fibrosis) were 0.850, 0.773, and 0.848, respectively. When the categorization was different among the reviewers, they discussed the issue until a consensus was reached.

Statistics

Statistical analysis was performed using JMP 10.0 software (SAS Institute Inc, Cary, NC). Continuous variables were expressed as the mean (SD). The χ^2 test and Fisher exact probability test were performed to analyze the correlation between parameters. Univariate and/or multivariate logistic regression analyses were conducted to identify parameters that significantly contributed to the primary and secondary outcomes. A $P < 0.05$ was considered statistically significant.

RESULTS

Comparison of Noncancerous Regions of the Pancreas in Patients With PDAC With Patients' Clinical Parameters

Fifty-five (72%) of the 76 cases showed positive fatty changes, 11 (14%) showed positive inflammatory changes, and 65 (86%) showed positive fibrotic changes. The correlations between